OCS Study
BOEM 2020-015

Coastal Marine Institute

A Real-time Ocean Observing Station Off Timbalier Island, Louisiana

Bureau of Ocean Energy Management

U.S. Department of the Interior
Bureau of Ocean Energy Management
Gulf of Mexico OCS Region

Cooperative Agreement
Coastal Marine Institute
Louisiana State University

OCS Study
BOEM 2020-015

Coastal Marine Institute

A Real-time Ocean Observing Station Off Timbalier Bay, Louisiana

Authors

Chunyan Li
Brian Milan
Eurico D'Sa
Wei Huang
Yixin (Peter) Luo

February 2020

Prepared under BOEM Cooperative Agreement M15AC00015
by
Louisiana State University
Coastal Marine Institute
Baton Rouge, Louisiana 70803

Published by

U.S. Department of the Interior
Bureau of Ocean Energy Management
New Orleans Office

Cooperative Agreement
Coastal Marine Institute
Louisiana State University

DISCLAIMER

Study collaboration and funding were provided by the US Department of the Interior, Bureau of Ocean Energy Management (BOEM), Environmental Studies Program, Washington, DC, under Agreement Number M15AC00015. This report has been technically reviewed by BOEM, and it has been approved for publication. The views and conclusions contained in this document are those of the authors and should not be interpreted as representing the opinions or policies of the US Government, nor does mention of trade names or commercial products constitute endorsement or recommendation for use.

REPORT AVAILABILITY

To download a PDF file of this report, go to the US Department of the Interior, Bureau of Ocean Energy Management Data and Information Systems webpage (http://www.boem.gov/Environmental-Studies-EnvData/), click on the link for the Environmental Studies Program Information System (ESPIS), and search on 2020-015. The report is also available at the National Technical Reports Library at https://ntrl.ntis.gov/NTRL/.

CITATION

Li C, Milan B, Huang W, Luo Y. A real-time observing station off Timbalier Bay, Louisiana. 2020. New Orleans (LA): US Department of the Interior, Bureau of Ocean Energy Management. OCS Study BOEM 2020-015. Cooperative Agreement No.: M15AC00015. 74 p.

Abstract

Offshore real-time oceanographic stations are difficult to establish, operate, and maintain. For one reason, the oceanographic conditions are not always favorable for instruments and most installation and maintenance work. For example, severe weather, bio-fouling, especially in the subtropical ocean environment of the Gulf of Mexico, metal corrosion in seawater environment, difficulty in access whether by ship or airplane, and high costs are all important factors. Another reason is that it is very difficult to mount any instrument in a fixed position in the ocean for long-term operation: oceans are deep, sedimentation can bury a bottom-mounted device over time, and the powers of winds and ocean currents make any installation of any equipment a daunting task. Indeed, there are very few real-time stations off the Louisiana coast on the continental shelf. The Wave-Current-Surge Information System has been operating a few such stations for metocean (meteorology and physical oceanography) data over the years. These stations are based on oil and gas platforms and are bulky. The stations are based on old computers and technologies and difficult to maintain. This project uses new technology: it does not use an onsite computer, it does not need a cooling system, it uses an omnidirectional small satellite antenna, and so is reliable and easy to maintain. We are the first users to work with the company who makes this system and there have been challenges. The system has collected 10 months of data and still operating. It would be beneficial if the system is duplicated; this would make the overall operation standardized and more cost effective.

Contents

List of Figures

List of Tables

List of Abbreviations

Short Form	Long Form
ADCP	acoustic Doppler current profiler
AOS	automated observing system
AWAC	acoustic wave and current sensor
CDOM	colored dissolved organic matter
CTD	conductivity-temperature-depth sensor
CSI	Coastal Studies Institute
FVCOM	Finite Volume Community Ocean Model
GCOOS	Gulf Coast Ocean Observing System
IOOS	integrated ocean observing system
SPM	suspended particulate matter
WAVCIS	Wave-Current-Surge Information System

1. Introduction

1.1 Data Need

One of the major challenges that we face in the northern Gulf of Mexico coastal area is the need for a better and reliable offshore metocean (meteorology and physical oceanography) real-time data collection system. Such a system will support the mission of the Bureau of Ocean Energy Management (BOEM) and other federal and local agencies engaged in coastal management, protection, and restoration, especially along the Louisiana coast. This area has a suite of environmental problems that require the acquisition of real-time data for immediate assessment or model based assessment and predictions that rely on this kind of data. This need was demonstrated by the 2005 hurricanes Katrina and Rita (Rego and Li 2010a 2010b), 2008 hurricanes Gustav and Ike (Li et al. 2009a, Li et al. 2010), the 2008 and 2011 Mississippi River flood diversions (Falcini et al. 2012, Kolker et al. 2014), and the 2010 *Deepwater Horizon* oil spill. One such system providing this kind of data is managed by the Wave-Current-Surge Information System (WAVCIS) at Louisiana State University (LSU).

WAVCIS, established in 1997, has been providing technical and operational services to one of the eleven regional associations of the US Integrated Ocean Observing System (IOOS) along the Louisiana coast, the Gulf Coast Ocean Observing System (GCOOS). These services are well in line with BOEM’s mission to “make decisions about the environmental risks and socioeconomic impacts of offshore oil and gas development in federal waters”, which require reliable information for weather and ocean conditions around the oil and gas production units. In addition, BOEM’s Marine Minerals Program manages non-energy minerals (sand and gravel) on the Outer Continental Shelf (OCS) for coastal restoration. “BOEM ensures that the removal of any mineral resource is conducted in a safe and environmentally sound manner, and that any potentially adverse impacts on the marine, coastal, or human environments are avoided or minimized”. For that purpose, offshore environmental data are crucial for the managers, engineers, and researchers.

WAVCIS has been an important component of BOEM’s Marine Minerals Program; it provides observational data for wave modeling validations associated with predicting impacts to wave climate associated with excavating offshore sediments. In addition to hurricanes, more frequent but less severe winter storms can also introduce significant hydrodynamics response (e.g., Feng and Li 2010, Li 2013, Li et al. 2011a, 2018, and 2019) and related sediment movement. The existing system, however, had been aging. The three working stations, Stations 3, 6, and 9, though the only such stations in the offshore area of the coastal Louisiana, were experiencing persistent technical problems due to a lack of funding, outdated electronic and data logging technology, and aging mechanical equipment. The present project was designed to develop a new system using new technology that would be more economical to operate and at the same time, more reliable, with better sensors and data loggers, as well as data transfer technology.

1.2 Coastal Waves and Currents

The fate of suspended sediment and related geomorphological changes–such as the land loss, evolution of dredged underwater pit after sand source excavations, oil spills, and nutrient transport–depends on the physical conditions of the coastal ocean, particularly waves, currents, and water levels. The physical conditions of the ocean, in turn, are affected significantly by the weather, such as. hurricane storm surges and winter storm surges during cold and warm front events. The weather impact and storm surge effects can be quite pronounced in the Louisiana area because of the low profile of the Louisiana coastal plain topography and shelf slope shaped by the Mississippi River and suspended sediment load over the geological time scales. According to Cochrane and Kelly (1986), the Texas-Louisiana shelf has an almost year-round east to west coastal current, except during the summer when the coastal currents may be reversed by wind regime changes.

Our recent analysis of the WAVCIS data has shown that the variability over the general coastal current described by Cochrane and Kelly (1986) and many others is highly dependent on the weather. Both waves and currents are variable, even though the general trend of the coastal current is mostly east to west. Short-time episodic weather impacts, however, can be quite significant, such as oil trajectories that are dependent on the history of the flows during an oil spill event. Further, many coastal geomorphological features have length scales smaller than the tidal excursion. The width of tidal inlets and the mouth of a bay in Louisiana are mostly smaller than the local tidal excursion. An episodic reverse of a coastal current could determine if an oil spill will enter into a bay or not. Figure 1.1 shows the water particle trajectories at various water depth measured from two offshore stations, Coastal Studies Institute (CSI) 3 and CSI 6, during the first month of 2008, indicating a few flow reversals due to wind shifts during winter storms (cold fronts). Such wind shifts can happen also during other times of the year (mid-fall to late spring, Walker and Hammack 2000). During the passage of cold fronts, increased wind speed usually causes long period of higher waves (Figure 1.2) that can cause significant sediment re-suspension (Figure 1.3, corresponding wind vector time series during that time period, Figure 1.4).

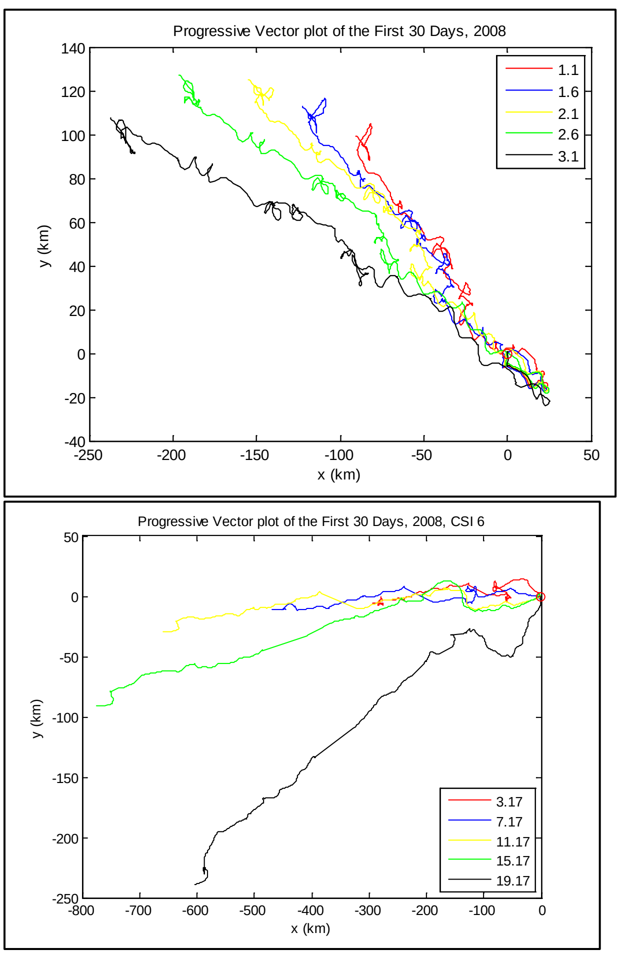

Figure 1.1. Vector trajectories from CSI 3 (left panel) and CSI 6 (right panel), Jan., 2008.

The colors and numbers in the inset indicate the distance of the data point from the sensor sitting at bottom. The unit for the depth of data with colored lines is in meters above the bottom.

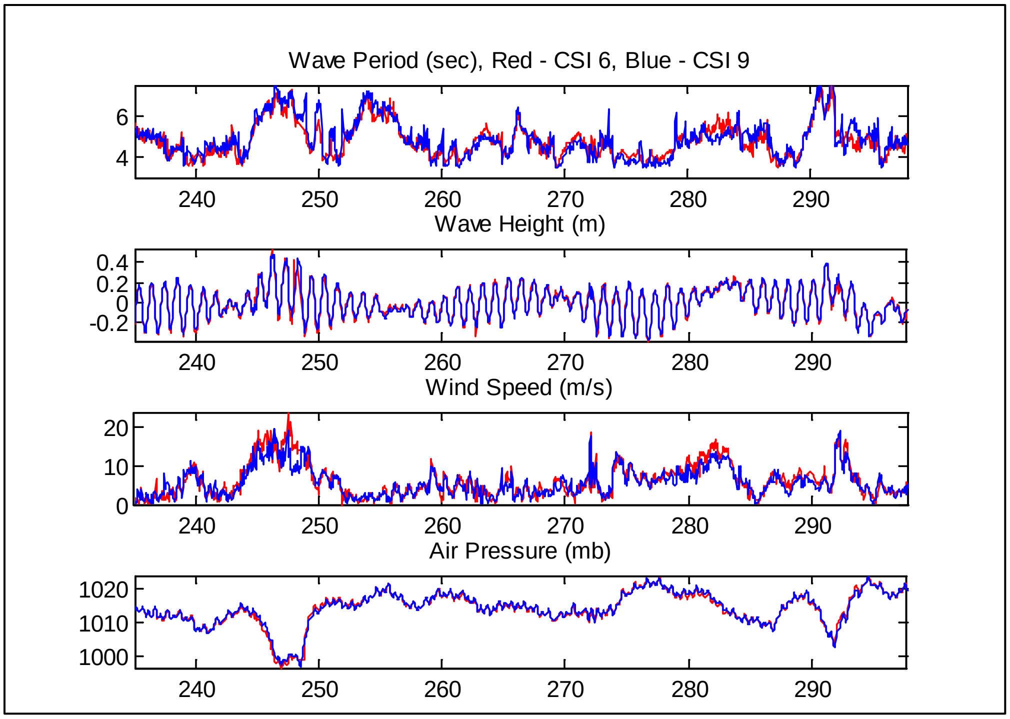

Time (days in 2008)

Figure 1.2. Wave period, water level, wind speed, and air pressure measured from CSI 6 and CSI 9 in 2008.

During a couple of strong wind events, wave periods are increased. The titles on top are the y-axis. The horizontal axis is time in days in the year 2008 (day 1 is Jan. 1, 2008).

Winter weather in Louisiana is dominated mostly by weather systems from the north and northwest. These weather systems are usually characterized by a low pressure center to the north of all the southern states, with a line of precipitation in parallel to a cold front trailing from the center of the low. The cold front is characterized by an air pressure minimum and a relatively sharp change of wind direction (from the southerly winds to northerly winds). The low pressure center forms a cyclonic circulation, often followed by a high pressure system behind the cold front, which is moving toward the south-southeast, before moving to the northeast. Though the low-pressure center of the cyclonic system is usually north of Louisiana and rarely reaches coastal Louisiana, the cold front formed along a trough of the low-pressure system often does sweep through the area. Another kind of cold front is a trough between two high pressure systems (the maritime tropical air and continental Arctic air) that is not obviously associated with a northern cyclone. In any case, the pre-frontal wind from the southern quadrants brings in relatively warm and wet air from the Gulf of Mexico, providing moisture and energy for the formation of thunderstorms and precipitation in general, along the cold front (Hsu 1988).

This kind of winter weather also occurs often during late fall and in the spring. The occurrence of cold fronts is a way for the atmosphere to exchange heat and redistribute thermal energy between high and low latitudes, by which the north-south temperature gradient can remain limited. Cold fronts are related to large scale atmospheric processes in which the westerly winds, set up by the north-south temperature gradient through geostrophic balance, has an important role. In the process, the atmosphere adjusts itself, tending to homogenize the air temperature, and cold air from the north needs to break through the barrier of the Jet Stream (the maximum zone of the upper troposphere westerly winds) to reach the south. As a result, the weather associated with a cold front can usually be identified by the upper level Jet Stream meandering toward the south. The frontal position is usually on the east of an upper level trough. As the mid-latitude Jet Stream meanders through the US, the associated cold front may sweep through the coastal Louisiana area.

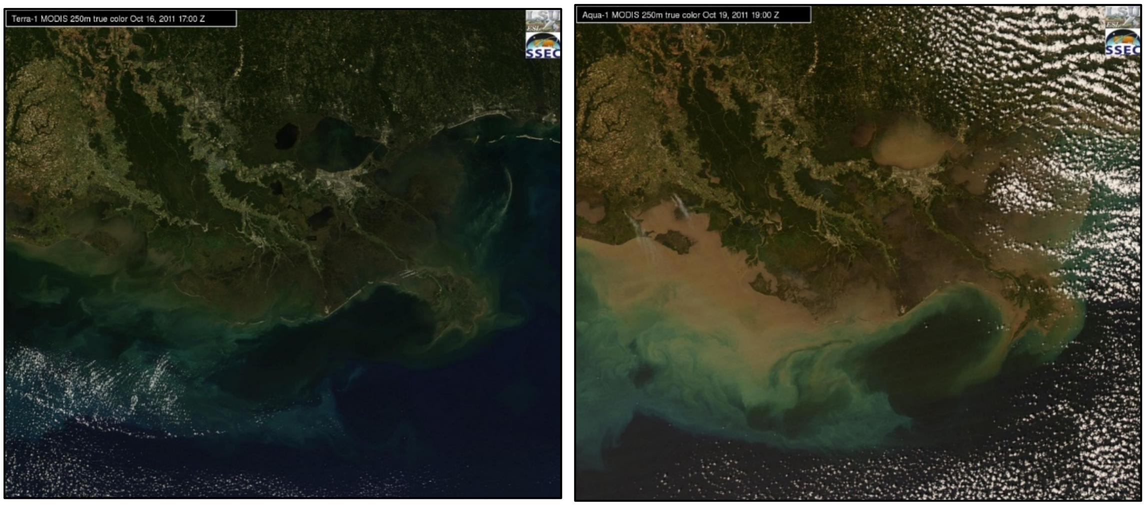

Figure 1.3. MODIS images showing suspended sediment along the Louisiana coast before and after a winter storm.

Left: Oct. 16, 2011; right: Oct. 19, 2011.

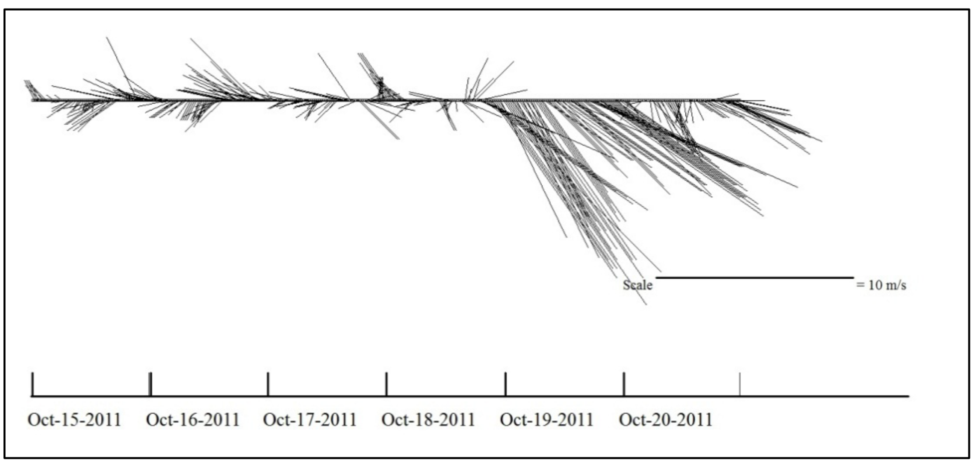

Figure 1.4. Wind vector showing the abrupt increase of wind on October 19, 2011 due to a winter storm.

As is documented (e.g., Roberts et. al. 1989, Walker and Hammack 2000, Feng and Li 2010), cold fronts occur at roughly weekly intervals. The pre-frontal winds from the southern quadrants bring up the water level in the coastal bays, lakes, and lagoons. This is often associated with high surface waves due to the long fetch of the southerly winds. As the front passes the area, the winds switch to those from the northern quadrants, which push the water level down. The contrast in wind directions causes a relatively large swing of the bay water (e.g., Li et al. 2011a, 2011b). As much as 40–50% of the water volume can be flushed in and out of a coastal Louisiana Bay during a typical cold front event (Feng and Li 2010).

The importance of cold front and its impact to coastal waters have been more appreciated by the coastal geologist but not by the majority of the physical oceanography community. The importance of cold fronts can be argued at least in three aspects: first, they occur frequently in the fall to spring seasons almost everywhere in the mid-latitude on our planet. Second, a cold front system has a much larger scale than any regional coastal oceanographic problems—it is an atmospheric event that has ~1000 km scales and thus affects a large area. A cold front can easily stretch over multiple states in the US mainland. Third, cold fronts occur every year at 3–10 day intervals (Feng and Li 2010; Li 2013; Li et al. 2008b, 2011a, 2011b; Li and Chen 2014; Lin et al. 2016). Coastal observing stations can be invaluable in providing continuous data that advances our understanding of the coastal currents in the area and the implications to coastal geomorphology under these quasi-periodic and recurring synoptic scale atmospheric events every year.

1.3 Sediment Transport

Several important issues about the Louisiana coastal water require understanding and quantifying the sediment transport, which is highly dependent on the weather and hydrodynamics. For example, the evolution of sandy barrier islands, the effectiveness and environmental consequences of coastal restoration engineering projects, and the protection of underwater pipelines of oil and gas industry where dredging activities to harvest sand can occur in a nearby area. In the offshore environment of a large river delta, both sandy deposit and muddy deposits exist. Coastal Louisiana's low profile land and wetlands are protected by many barrier islands. The wetlands, however, are experiencing net loss at a rate surpassing other places in the US. These barrier islands are sandy sedimentary environments separated from the mainland by estuary or lagoon environments. The barrier islands protect interior estuaries and wetlands from weather forcing, waves, and storm surges. A major component of the State of Louisiana's effort to manage coastal land loss is to restore degraded barrier shorelines by dredging sand from borrow sites and delivering it where it is needed. Dredging the bottom to harvest sand can impact the sea floor and its surrounding environments, and is a subject of study for oceanographers, engineers, benthic ecologists, archeologists, environmental scientists, and decision makers. How a dredged site evolves depends greatly on the physical forcing and hydrodynamics. About ninety percent of the Mississippi and Atchafalaya rivers' sediment load is suspended mud, with sediment finer than 63 μm in diameter, and only about ten percent is sand (Nittrouer et al. 2008). Thus sand resources are quite scarce. Excluding the far-offshore sand deposit sites, the economic sand resource near the coast is even more limited. Understanding the spatial and temporal variations of the formation of limited sand resources along the Mississippi Deltaic Plain is critical to the success of dredging projects. Further, the suspended particulate matter (SPM), a large fraction of which is composed of suspended sediments along the river-dominated Louisiana coast, strongly influences the light field and thus primary production and the ecology of the region. In addition to the rivers, dredging, sedimentation, and physical processes (e.g., currents, waves) will influence its transport and budget, necessitating regular monitoring to detect changes due to both natural and human impacts. Because in situ measurements of SPM are time consuming and expensive, optical scattering methods provide an alternative for more continuous observation of SPM. Field observations have shown good relationships between optical backscattering and SPM in various coastal environments (Zawada et al. 2007), including the Louisiana coast (D'Sa et al. 2007; Figure 1.5 upper panel). Ocean color or spectral reflectance of the ocean is, at the first-order of approximation, proportional to optical backscattering (Boss et al. 2005) allowing for the development of ocean color algorithms for SPM from optical measurements (Figure 1.5 lower panel, D'Sa et al. 2007). The integration of an optical backscattering sensor at the selected site would provide an important optical proxy for suspended sediments that would be used to monitor changes in SPM in conjunction with physical forcing, as well as for examining trends in ocean color observations related to SPM (D'Sa et al. 2007, 2008; Zawada et al. 2007).

A conceptual model of sediment deposition under both regressive and transgressive environments was proposed by Penland et al. (1989). Prograded deltaic headlands are reworked by marine processes, often influenced by weather, after river abandonment, resulting in transgression and transformation to ebb tidal delta and before becoming an inner-shelf sandy shoal. The majority of the northern Gulf of Mexico is dominated by muddy deposits and only a fraction of restoration-quality sand is located nearshore. These include Tiger Shoal, Trinity Shoal, and Ship Shoal. However, these are located south of Atchafalaya Bay, which makes it too costly to use in most restoration projects. On the other hand, discrete sand deposits associated with ancient rivers that flowed across the shelf during the earlier stages of shelf and delta evolution did occur close to shore within the OCS area. As sea-level rose, these channels were filled with sandy sediment and ultimately buried by more recent muddy deposits from the modern rivers. Suter et al. (1987) identified numerous incised fluvial systems offshore of the western Louisiana Chenier Plain. These river channels were widely distributed along 800 km-long Louisiana coast and were formed in geological history when the sea levels fluctuated and the rivers switched lobes. Some of these paleochannels are close to the modern shorelines. These channel-filling sands on the continental shelf have been targeted for coastal restoration projects, resulting in significant cost savings. In 2014, BOEM contracted a Louisiana State University (LSU) team to study the fate of mud-capped dredged pits at several offshore sites, including one near Raccoon Island (Figure 1.5) (Zhu et al. in press). In the future, this kind of project will rely on environmental data that can provide information for the study of the fate of mud-capped dredged pits, the impact to its environment, the evaluation of the appropriateness of existing safety distance to nearby pipelines, and management of resources and policy assessment and regulations.

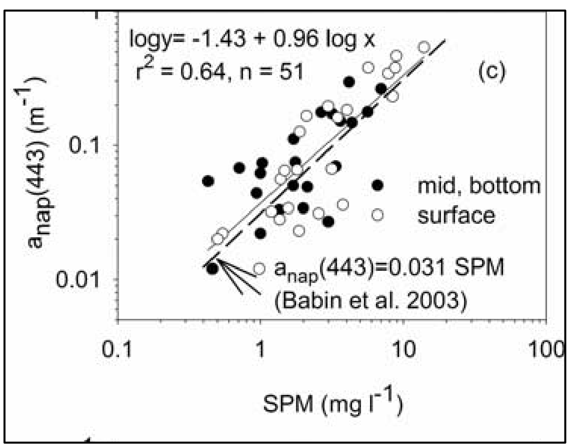

Figure 1.5.a. Relationship between suspended particulate matter (SPM) and optical backscattering obtained at various locations during field sampling along the Louisiana coast.

The variable a_{nap} is the nonalgal particle absorption.

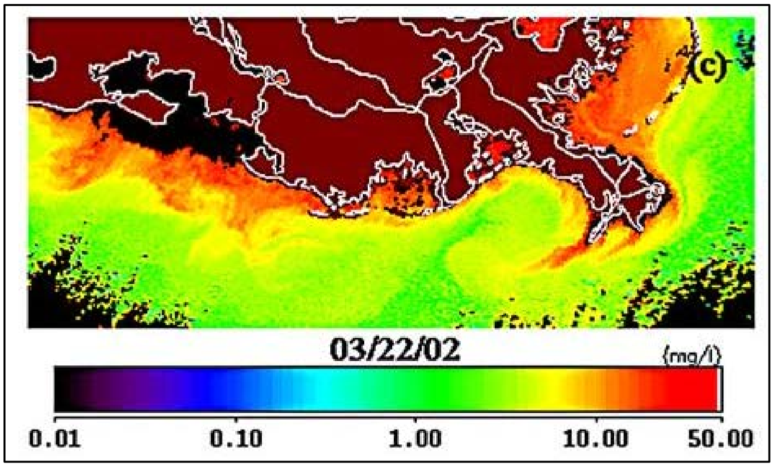

Figure 1.5.b. Lower panel: SeaWiFS satellite derived imagery of SPM (mg/L) obtained using a regional algorithm (figure from D'Sa et al. 2007).

1.4 Objectives

Originally, our main objective for this project was to revive and significantly upgrade the old WAVCIS station CSI 5 for high quality, continuous, and real-time metocean data collection and sharing. The actual station is not CSI 5 but SS91 or the Station 10 of WAVCIS at (28.92ºN, 90.77ºW). The system is more efficient and reliable as new technology for power system (including cooling system which is needed for this subtropical marine location). In addition to the real time continuous ocean velocity profile observations, we also install an optical backscatter sensor, on a short-term basis (not providing real time data). The time-series optical measurements will enhance the ocean data collection to support decision making related to environmental conditions and sediment transport that could affect environmental conditions in the proposed study area. The optical measurements will also support efforts to improve ocean color satellite estimates of these environmental parameters in optically complex coastal waters (D'Sa et al. 2006, 2008, 2011, 2014). With the establishment of this WAVCIS station at SS91, the system no longer uses the old desktop computer on site like the other existing WAVCIS stations do. Instead, we use a new satellite transmission system that is more reliable and without the need of a cooling system that is prone to problems. As a result, the power needs will be much less. This change also eliminates all software upgrades frequently needed for the desktop Microsoft Windows®-based computers, which caused security problems and impacted the effective speed of data transfer.

We also eliminated the external data loggers. Our old external data loggers were based on technology more than 10 years old. They were not designed for the amount of data traffic with many sensors and frequent samplings. As a result, it became slower in data transfer as more sensors were added. Cheaper, faster, smaller, and more reliable data loggers integrated with the devices are now available and such an upgradecan benefit the entire program. It costs less as we reduce the number of required trips to the site for maintenance because with new technology, the system is more reliable and has more capacity in data storage.

Specific objectives of the project:

1) Establish a new real-time coastal observing station within the GCOOS network; this new station is outside of the Terrebonne-Timbalier bays. The station collects real time oceanography data and seasonal ocean optics data.

2) Collect real-time oceanographic data from this new station using new technology. The station will be maintained to have as much continuous data as possible. With the use of new technology we will no longer use the on-site Microsoft Windows®-based computer that often presented problems due to frequent automated upgrade and unnecessary overhead of various background programs that are not needed for the operation of the station.

3) Collect seasonal optical scattering data at the new station to assess temporal variability in suspended particulate matter and its physical linkages. Water samples will be obtained on site for suspended matter concentration.

4) Provide data and results from our analysis that will assist the other projects for mud-capped dredge pit evolution and enhance our understanding of mud-capped dredge pit evolution.

5) Help the implementation and improvement of regional coastal ocean models using Finite Volume Community Ocean Model (FVCOM) incorporating data from both the new station and nearby GCOOS stations for a better understanding of the physical factors on the sediment transport, coastal currents, water particle trajectories (for application on oil spill and pollutant transport) and evolution of dredged pit under various weather conditions. A series of numerical models have been developed in our labs and within the regional community funded by the Northern Gulf Institute, National Aeronautics and Space Administration (NASA), the National Oceanic and Atmospheric Administration (NOAA), BOEM, the State of Louisiana, and BP (for oil spill). Our data will be available online and accessible by the general public through the GCOOS, NOAA, and WAVCIS web pages.

1.5 Station

After a request from BOEM and subsequent discussions, we originally selected the old CSI 5 station as the site for the new system, which is located in the proximity of the Ship Shoal sand body offshore Louisiana where dredging under BOEM's purview had been underway. Observations from Station CSI 5 were used in BOEM-funded studies to model potential environmental impacts associated with dredging (Stone et al. 2009); the results were used by BOEM for decisions and consultations with other resource management agencies. The idea was that with CSI 5 being inoperable, there would be no long or short- term wave or current observations available during the time when collecting those data would be critical: when dredging was actually occurring. In addition, post-dredging data could be used to validate any predictive model and inform future management decisions.

However, it was later determined that Station CSI 5 was not the best site for the kind of information needed. After an extensive search and discussion, as well as legal requirements (property use permit, boarding pass, etc.) with oil and gas companies, we selected a site off Timbalier Bay on Ship Shoal (Station 10A for WAVCIS).

2. Station Selection, Instrument, and Installation

2.1 Site Selection

Originally, the site for the new station was selected to be at the old CSI 5 (Figures 2.1, 2.2), which is an unmanned platform that was used by Wave-Current-Surge Information System (WAVCIS). It was later determined that this station would be too close to shore and far away from the area of interest (e.g., Ship Shoal) and a search for a proper site began. For instance, we examined a possibility of using a platform from Block 84, 86, 87, or 99. The purpose was to select a relatively new site that would not be decommissioned soon, allowing us to collect sufficient data. We also looked into the possibility of finding a wooden piling, which turned out to be very difficult to find. We identified a few locations that all turned out to be unsuitable for the project: most of the potentially good sites were to be decommissioned soon. At one point, a US Coast Guard lighthouse was identified as a potential site. However, it was later determined that the condition of the lighthouse was not favorable and at the same time there was an issue of the ownership. All these challenges delayed the project for about a year. By November 2016, we had been working on a boarding agreement with the owner (Fieldwood Energy) of the selected platform (Ship Shoal 91, 28.919ºN; -90.774ºW, Figure 2.3): we were in communication with people at Fieldwood Energy SS91, regarding a site visit before putting an acoustic Doppler profiler (ADCP) and conductivity-temperature-depth sensor (CTD) at the site.

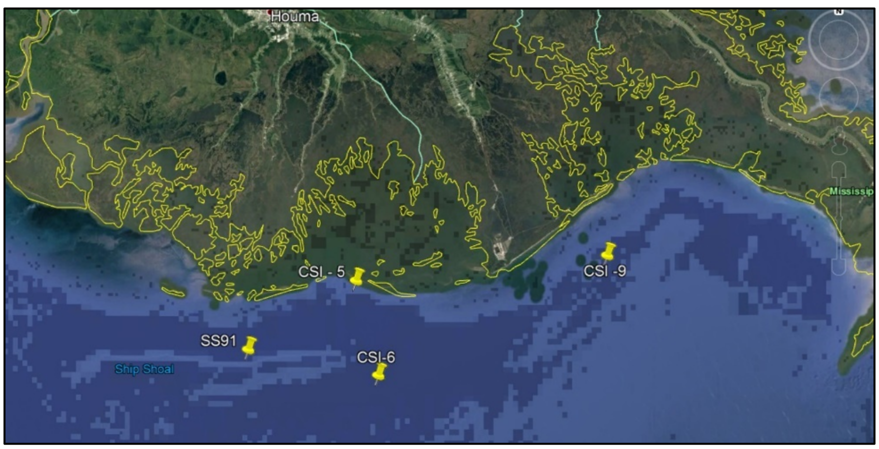

Figure 2.1. WAVCIS Stations and the new station (SS91).

The boarding agreement with Fieldwood Energy SS91 was approved by both Louisiana State University (LSU) and the company on December 12, 2016. After this, we were allowed to visit the site for measurements aimed at the design of the installation, and for the actual instrument installation after the manufacturing of the large clamps for fixing the conduit for cables.

The site SS91 at a shallow water depth of ~37 ft is ideal because (1) it is on Ship Shoal where dredging sand has been ongoing and (2) there is a need for proper assessment of the fate of a dredged pit under various weather and oceanographic conditions and (3) the integrated effect over the years. A real-time station for continuous measurements of oceanographic conditions will be valuable. This site is close to other WAVCIS stations (CSI 6 and CSI 9, e.g. Figure 2.4). This site is also in the coastal current zone throughwhich the Louisiana-Texas coastal current passes. It is also in the area of the seasonal hypoxia. The data from this site can be very useful for coastal current model validation. This kind of model can be used for many purposes, including the effects of severe weather, hypoxia, and oil spills, just to name a few.

Figure 2.2. CSI 5, the originally selected site.

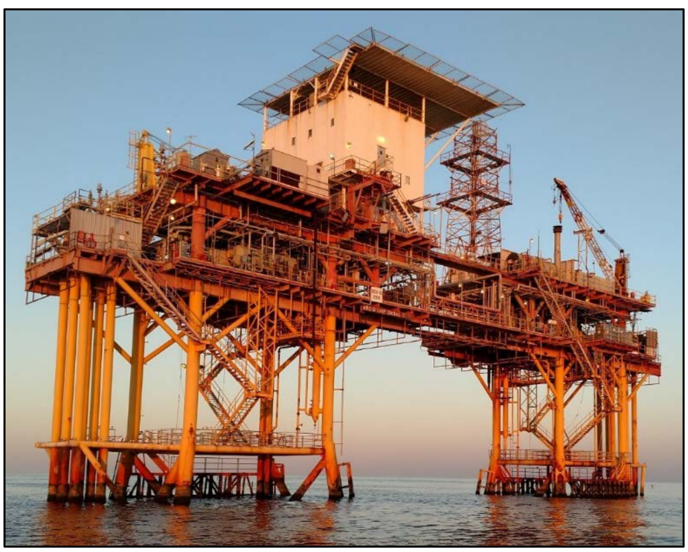

Figure 2.3. The final site, Fieldwood Energy on Ship Shoal 91 (SS91) A and B platforms (7 nm offshore).

Figure 2.4. A nearby station, CSI 6.

2.2 Instrument

To measure the current velocity profiles, we use the Nortek 1 MHz acoustic Doppler profiler (ADCP, Figure 2.5)–the 4-beam acoustic wave and current sensor (AWAC). The AWAC ADCP was *custom made* based on our request that the four transducers not be symmetric: they are facing one side so that no beam would be interfered with by the oil platform structure. To reduce biofouling, we painted the surface of the ADCP with blue color antifouling paint.

Figure 2.5. Custom-made ADCP to reduce the effect of the rig legs by facing the transducer sideways.

The blue color is antifouling paint that applied before the deployment.

The ADCP has a secure digital (SD) card for up to 4 GB of data storage. It is connected with the satellite transmission box (the Automated Observing System, or AOS Iridium Nortek module).

This AWAC ADCP at the new WAVCIS Station SS91 is a current profiler and a wave directional system in one unit. Traditional WAVCIS stations had ADCPs and separate pressure sensors that needed to be replaced yearly. Extra cabling was needed, as well. The SS91 ADCP can measure the current speed and direction in one-meter thick layers from the sensor depth to the surface. Waves of all varieties are measurable; this includes long waves, storm waves, short wind waves, or transient waves generated by local ship traffic. The customization of the ADCP heads allows for beams to gather data away from influence of rig structure. Traditional ADCP would have only one beam and it would be influenced by the oil rig's structure.

Figure 2.6. The new WAVCIS station antenna.

10" x 8" footprint; no cable needed; Iridium satellite omnidirectional antenna would not lose signal and data during and after strong wind events because the movement of the antenna does not affect the connection with the satellites.

Figure 2.7. Old WAVCIS station antenna.

96" x 72" footprint, hundreds of feet of coaxial cable to computer; subject to misalignment from strong winds.

The AOS data collection and/or transmission unit is designed for easy use and can handle harsh environments. The data collection unit is equipped with an Iridium satellite communication modem for a truly global coverage. It is a very small and light unit–only 10 x 8 inches (Figure 2.6), compared to the old WAVCIS antenna of 96 x 72 inches (Figure 2.7). It takes much less deck space, which is always very valuable on offshore platforms. In addition, because the old WAVCIS antennas are directional, they have to be precisely facing the direction of the geostationary satellite for reliable data transmission. In severe weather, the antenna might be moved by strong wind and data connection lost. The AOS system is omnidirectional and can be set in any orientation and not affected by strong wind during a severe weather. This makes the data transmission more reliable and the data quality higher.

The old WAVCIS ADCPs were all powered by on-site AC power from the oil and gas company that provided the platform. This new ADCP is powered by a solar panel-charged battery. This battery is securely housed in a weatherproof aluminum electronic box with an automated breaker that will click off when power surges or lightning strikes to stop the current going to the instrument and causing damage. This kind of box has been used by the US Department of Transportation along highways and is very reliable for outdoor use, including offshore deployment. The AWAC ADCP, solar panel, battery, cable, and the breaker installed battery box are shown in Figure 2.8. The ADCP is mounted at about seven meters below the surface and looking upward so it can record velocity profiles at hourly intervals.

Figure 2.8. The AWAC ADCP, solar panel, battery, cable, and the breaker installed battery box.

The battery box with the breaker and the AOS system are mounted on a panel that is vertically placed on the platform for data collection (Figure 2.9).

In addition to the ADCP, we also use a Seabird Electronic (SBE) CTD model SBE 37 SM (Figure 2.10). This is for the seasonal measurements together with the optical measurements and so there is no real-time data transmission from this instrument.

The optical instrument used is an ECO BBFL2 (WETlabs, Inc.) that is used mainly to measure optical backscatter at 700 nm (measurement range 0 to 3 m^{-1}). The instrument also includes measurements of chlorophyll-a fluorescence (measurement range 0 to 30 ug Chl/L) and colored dissolved organic matter (CDOM) fluorescence (measurement range 0 to 375 ppb). The instrument has internal memory capabilities, an anti-fouling wiper with copper faceplate, and internal batteries. The instrument was set up for a sampling period of 15 mins (96 samples/day) that could support data collection for a period of about four months. However, wiper movement potentially affected by fouling in the faceplate could reduce the sampling period. Before the deployment, the instrument was taken on a field trip and calibrated for suspended particulate matter and CDOM. Calibration was conducted by obtaining a series of optical measurements with the BBFL2 in surface waters in a Gulf of Mexico estuary. Concurrently, water samples were collected for measurements of suspended particulate matter (SPM; mg/L) and CDOM absorption coefficients (m^{-1}).

Figure 2.9. The mounting panel installed at the SS91 platform with battery inside the housing on the left and the AOS on the right.

Figure 2.10. Conductivity-temperature-depth sensor deployed at SS91.

The third piece of equipment deployed at SS91 is a WETLabs Eco scattering sensor. The ECO-w comes with an active anti-biofouling design for longer-term mooring deployments. The ECO-w is programmed to sample at hourly intervals; data is stored onboard its memory. Time series of the optical data are used in conjunction with physical measurements to obtain a mechanistic understanding of the seasonal variability of suspended material at the site.

2.3 Design of the Installation

The design of the installation was made by the technicians at the Field Support Center, Coastal Studies Institute at LSU. The major pieces include: (1) the conduit, partially submerged, for cable that sends data up to the deck unit AOS system for satellite data transmission; (2) the clamps for fixing the conduit on one of the platform legs; and (3) a mounting structure for the instrument package (the ADCP, CTD, and ECO-w). The engineering drawing for the system is provided in Figures 2.11–2.18.

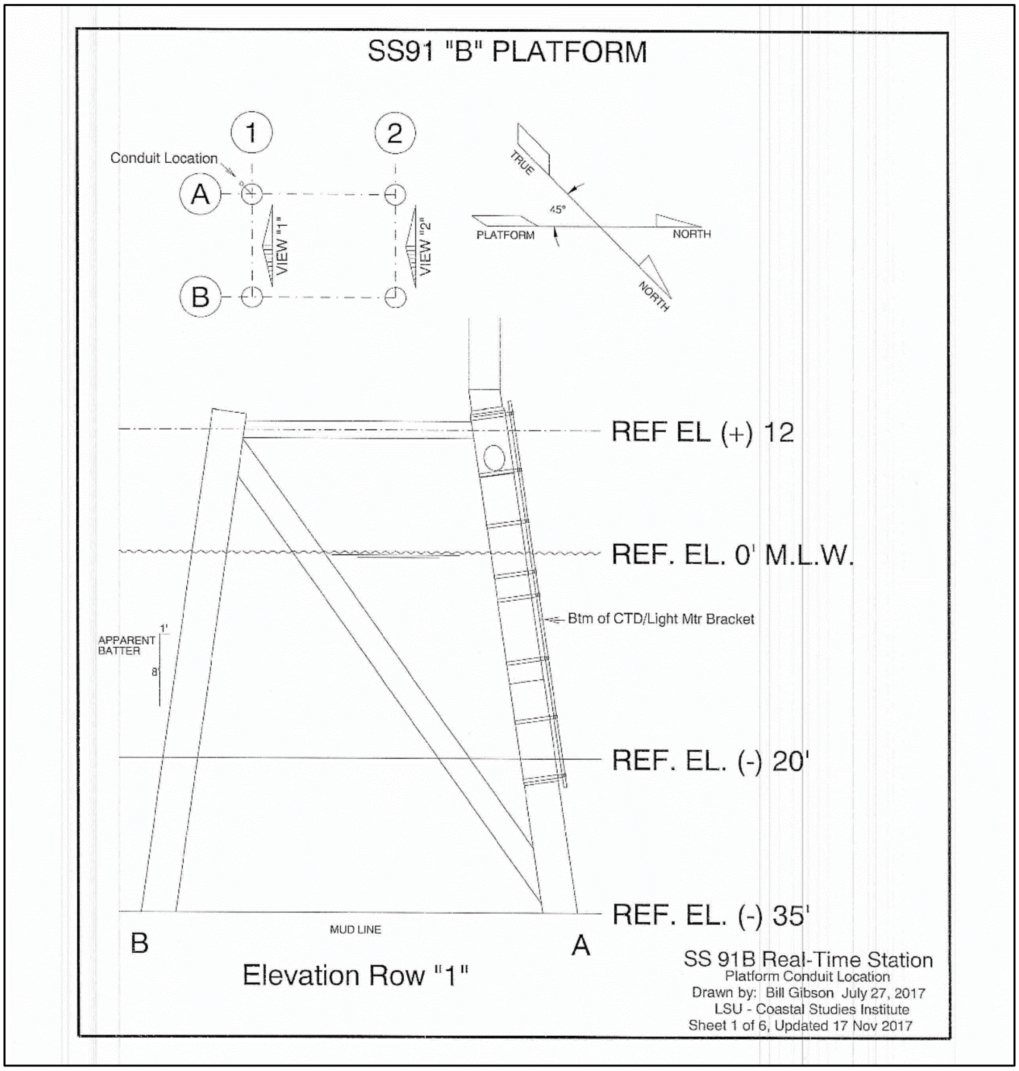

Figure 2.11. Engineering drawing (1) for the installation at SS91.

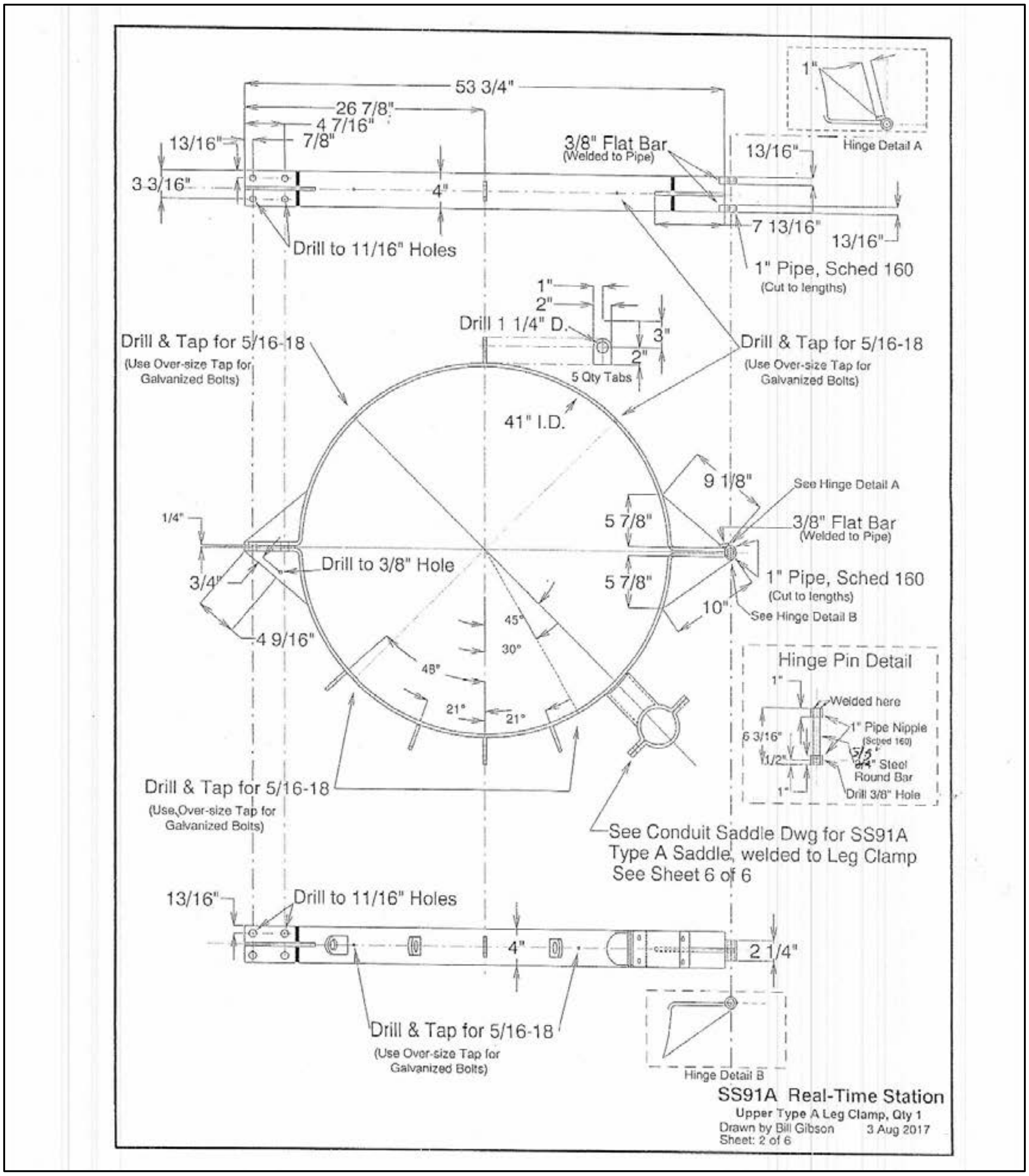

Figure 2.12. Engineering drawing (2) for the installation at SS91.

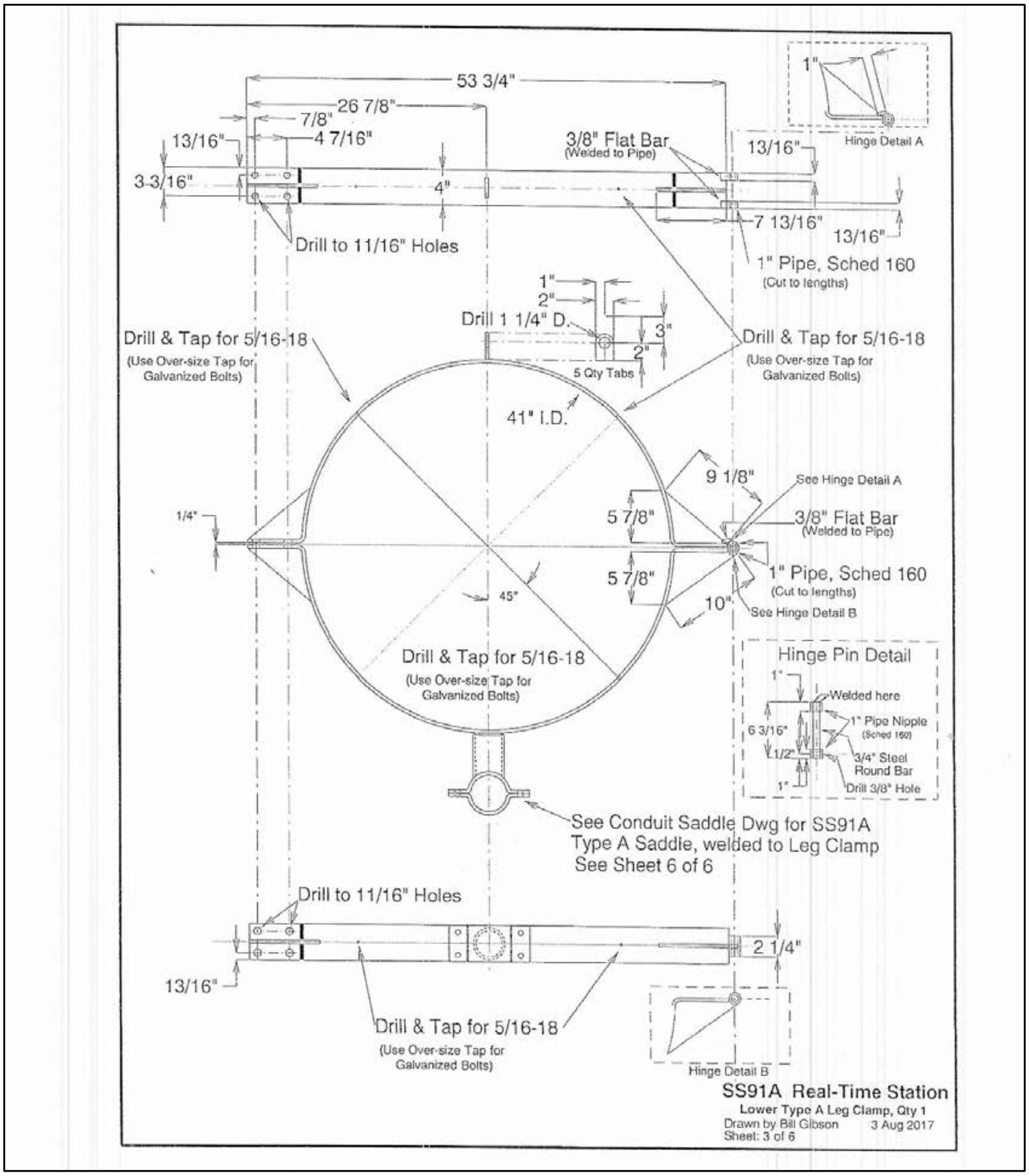

Figure 2.13. Engineering drawing (3) for the installation at SS91.

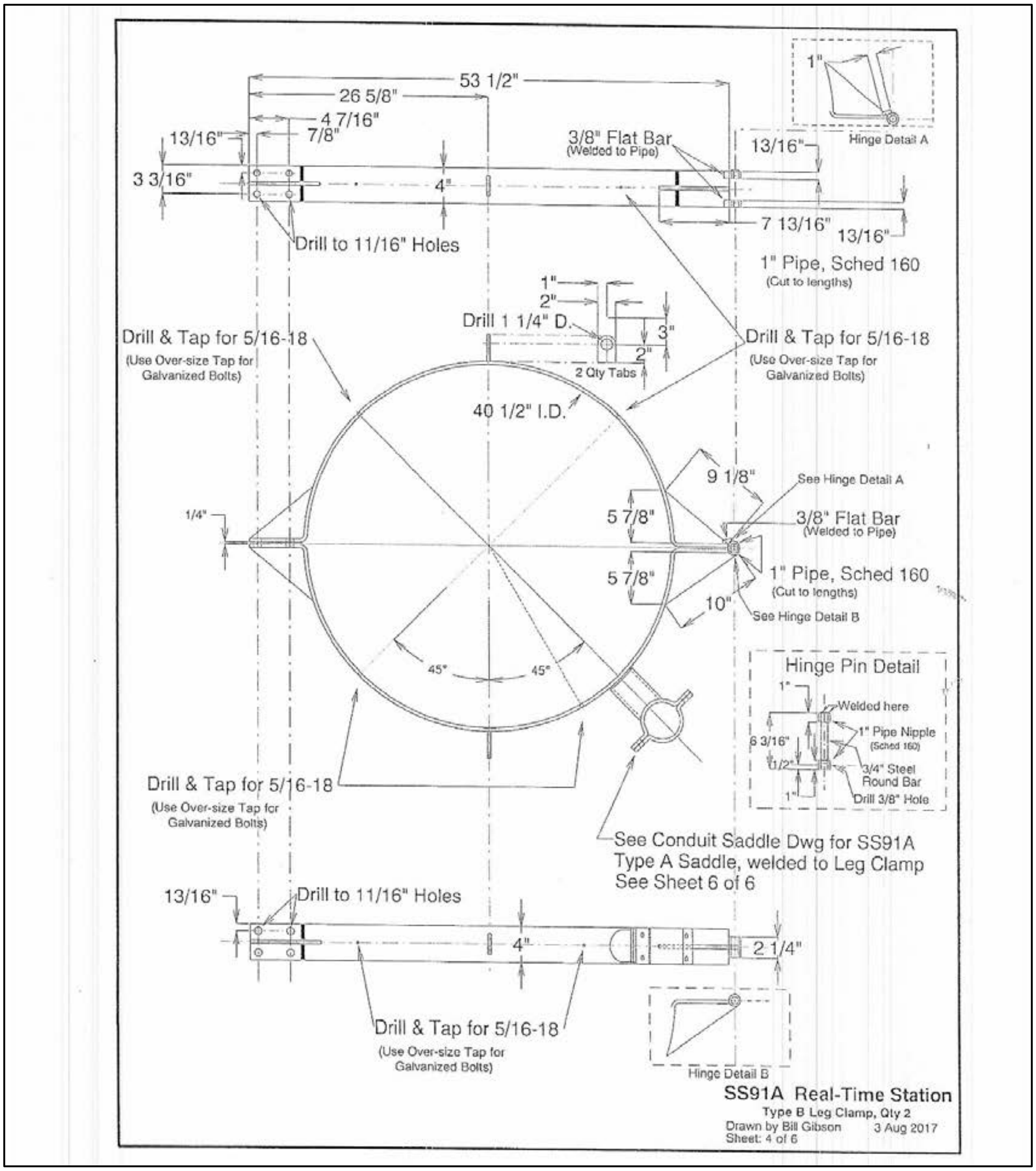

Figure 2.14. Engineering drawing (4) for the installation at SS91.

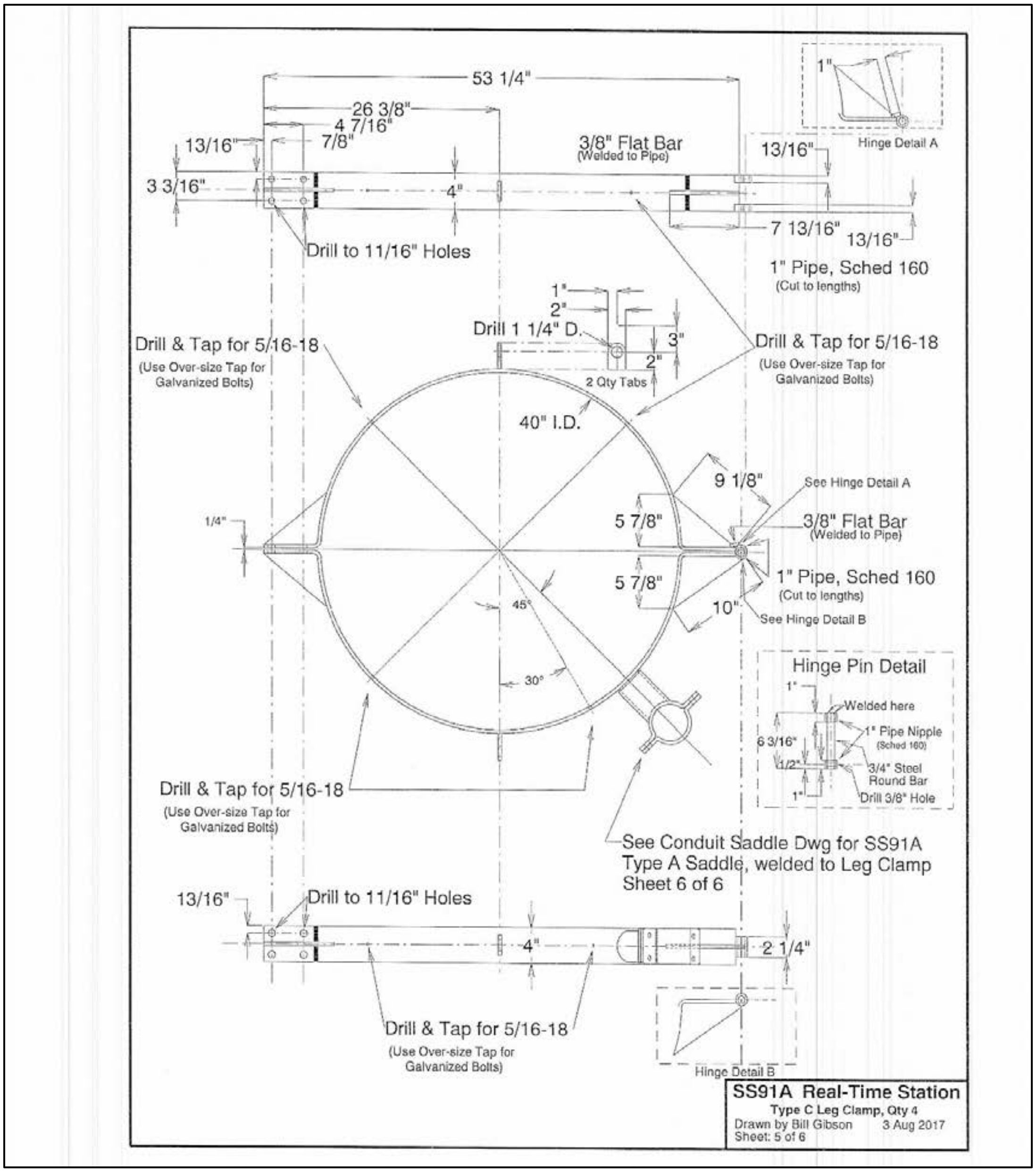

Figure 2.15. Engineering drawing (5) for the installation at SS91.

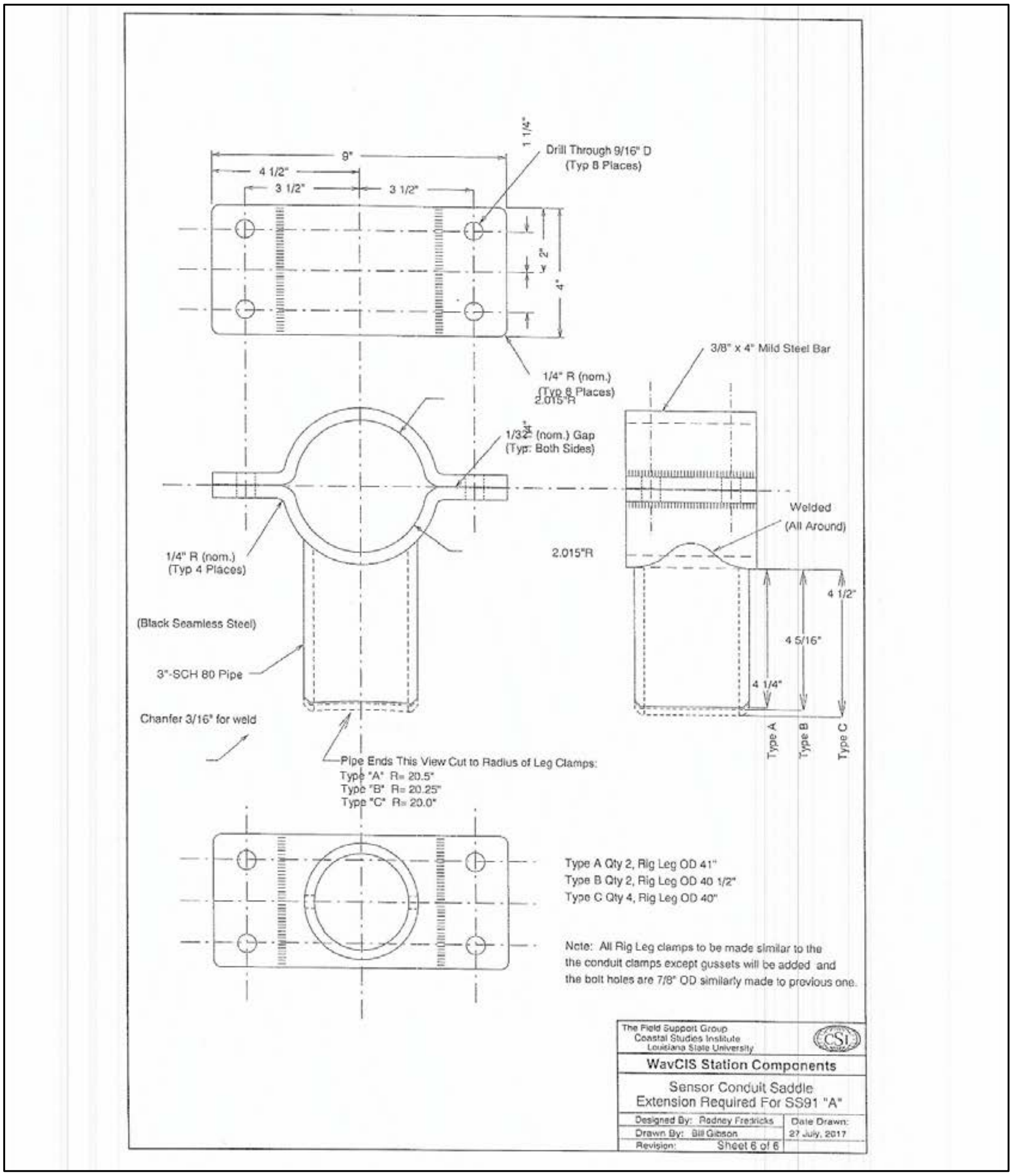

Figure 2.16. Engineering drawing (6) for the installation at SS91.

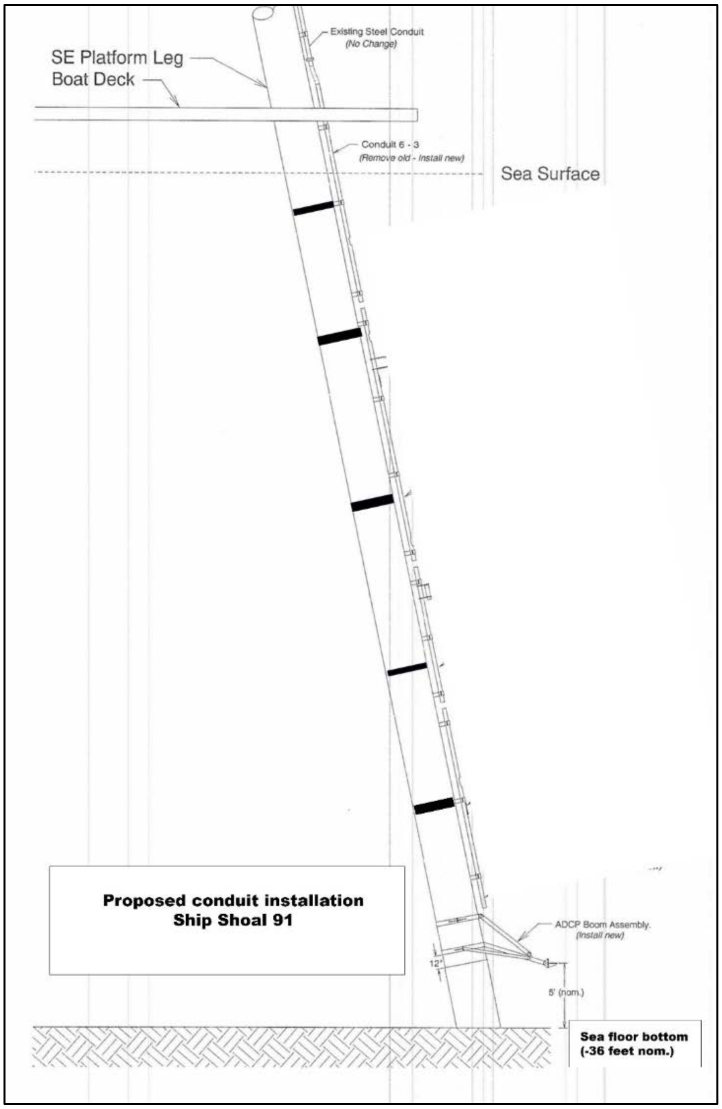

Figure 2.17. Conduit installation on one of the rig legs.

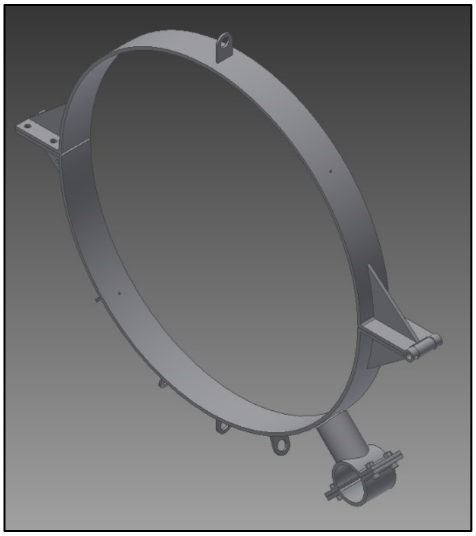

Figure 2. 18. CAD drawing of the clamp for the conduit.

2.4 Test Installation and Test Run of the System

Before the actual installation and operation of the new station at SS91, we had two test installations and test runs at two inshore stations: one at the Caminada Pass between May 25, 2014 and January 2, 2016 (we call this the pre-project test), and the other at Barataria Pass between March 16, 2017 and April 4, 2018 (we call this project test). Figure 2.19 shows the installation at the latter.

Figure 2.19. Test station at Barataria Pass for the AOS system before the actual deployment at SS91.

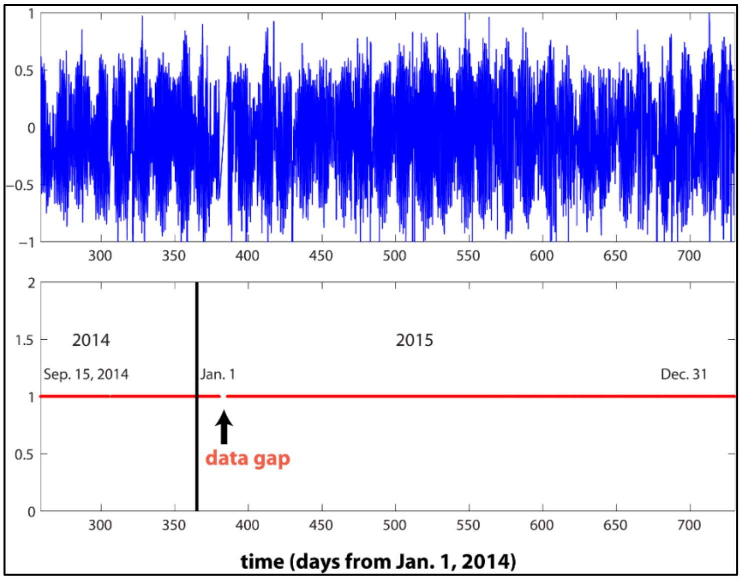

Figure 2.20. Example velocity data from the entire period of the first test run at the Caminada Pass.

The upper panel shows the north velocity component from one bin; the lower panel shows the data inventory.

The test installations and operations were a great success. With the first installation as an example, from September 15, 2014 to December 31, 2015, data were almost continuous except two gaps when the battery went low (Figures 2.20–2.21). At that time, the AOS box used only batteries but was not connected to a solar panel yet and the replacement of battery required a manual onsite service.

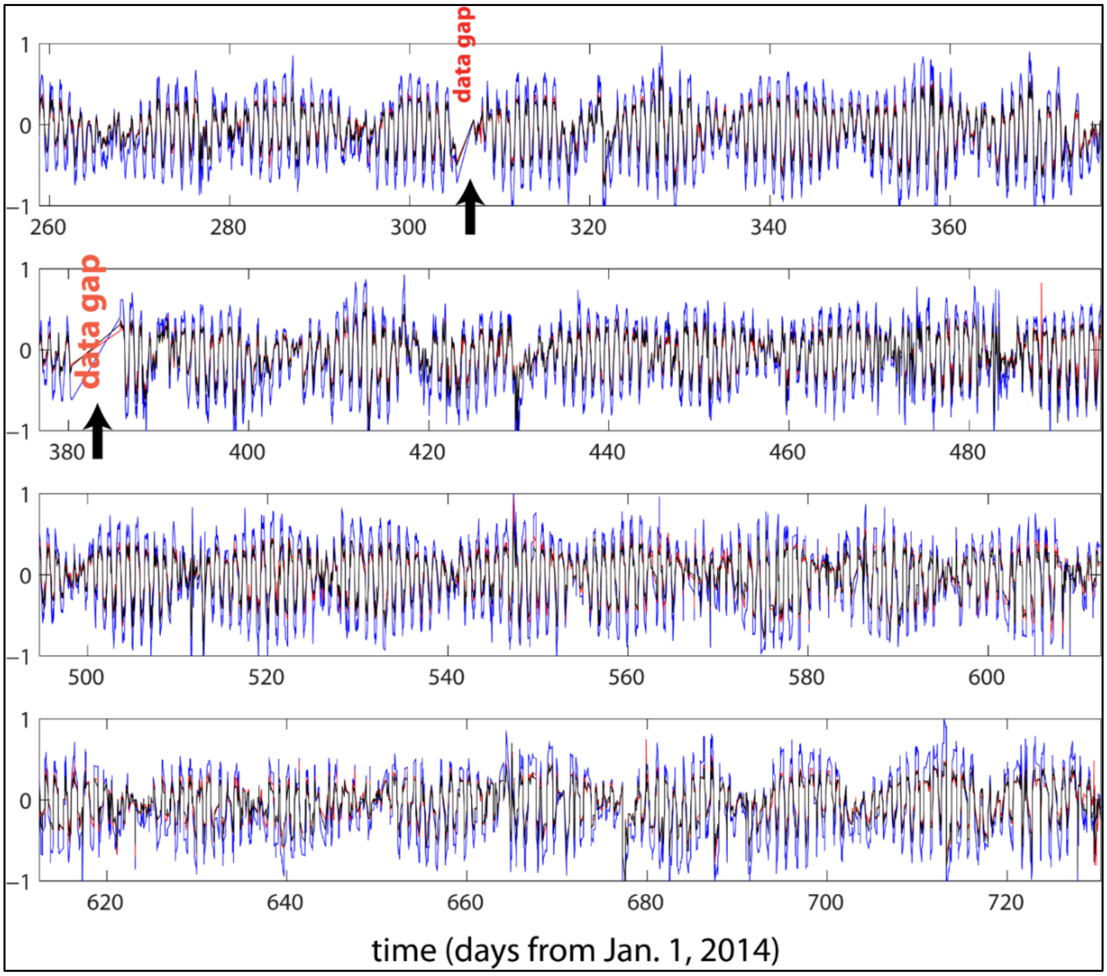

Figure 2.21. Zoomed in flow velocity data for bins 5, 10, and 20 (shown by 3 different colors).

From September 15, 2014 to December 31, 2015, data were almost continuous except two gaps when the battery went low.

2.5 Installation

After all the preparations, and some delays due to weather and ship time scheduling issues, the new station at SS91 was finally finished with several trips and the AWAC AOS system started recording real-time data from August 23, 2018 and still functioning at the time of this report. It should be noted that the instrument operated in real time from August 23 to December 9, 2018 when it stopped because we were working with the system to optimize it and testing for a better position for the AOS box. There were some issues involving the cable: it must be explosion proof, which was a new regulation implemented after our proposed work. All the cables had to be remade. After working with the company, fixing issues of data transmission, we boarded SS91 again on March 2, 2019 when we fixed the problem onsite and reactivated the real-time data transmission for the AWAC ADCP. The data have been flowing real time since then. Figures 22–23 show the installations on SS91. We will discuss the data obtained so far in the next chapter.

Figure 2.22. The new station (SS91).

Shown in the picture are the locations of the AOS unit before March 2, 2019.

Figure 2.23. Photo of an installed clamp.

3. Data Collected

3.1 The Real-time Oceanographic Data

Data Inventory. As described earlier, after the whole system was installed and after a period of tuning and testing, the real-time data started to flow on August 23, 2018. The data stream stopped between December 6, 2018 and March 2, 2019, after which the system has been operational (real-time data collection continuing, Figure 3.1). Our last download of the data was on August 5, 2019 and our graphs of the data are all up to this time, even though the data are still being collected in real time.

Battery Voltage. The data are shown on the Wave-Current-Surge Information System (WAVCIS) web site and the post-processed data are to be regularly sent to the Gulf Coast Ocean Observing System (GCOOS). Between August 23 and December 6, 2018 the AOS used a non-chargeable battery and was not yet connected to the solar panel charged battery. As a result, the battery power declined gradually (Figure 3.2). After March 2, 2019, the solar panel powered battery was connected to the system and the battery voltage stayed pretty much stable; no obvious drop was seen (Figure 3.3). The oscillation of voltage shown in Figure 3.3. was caused mainly by the nighttime slight drop in voltage.

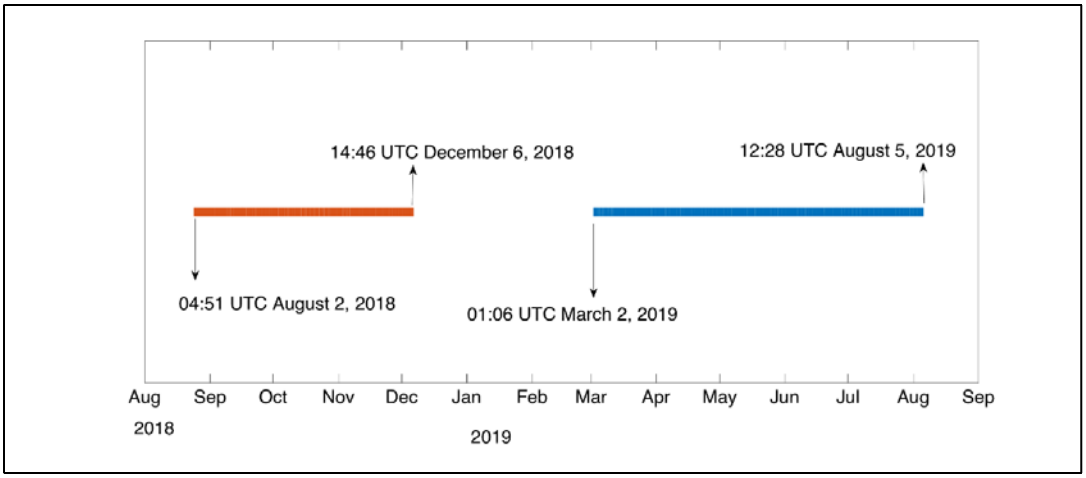

Figure 3.1. Data inventory for the SS91 acoustic wave and current sensor (AWAC) acoustic Doppler profiler (ADCP) data.

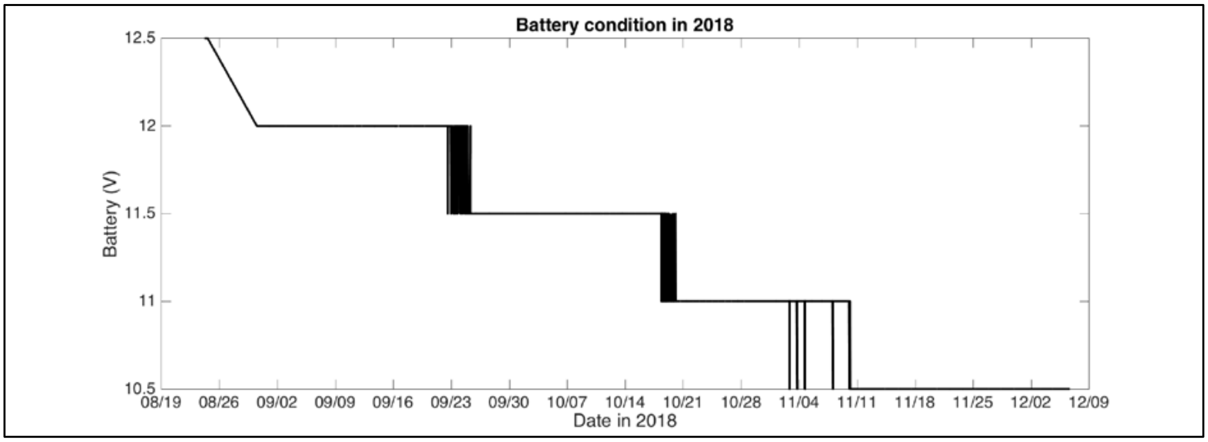

Figure 3.2. Time series of battery for the ADCP AOS system before December 6, 2018.

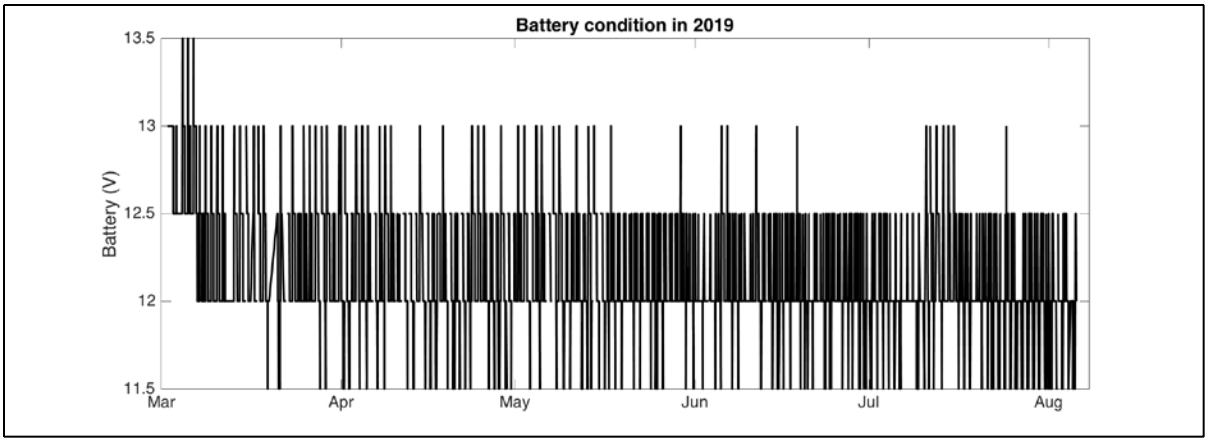

Figure 3.3. Time series of battery for the ADCP AOS system after March 2, 2019.

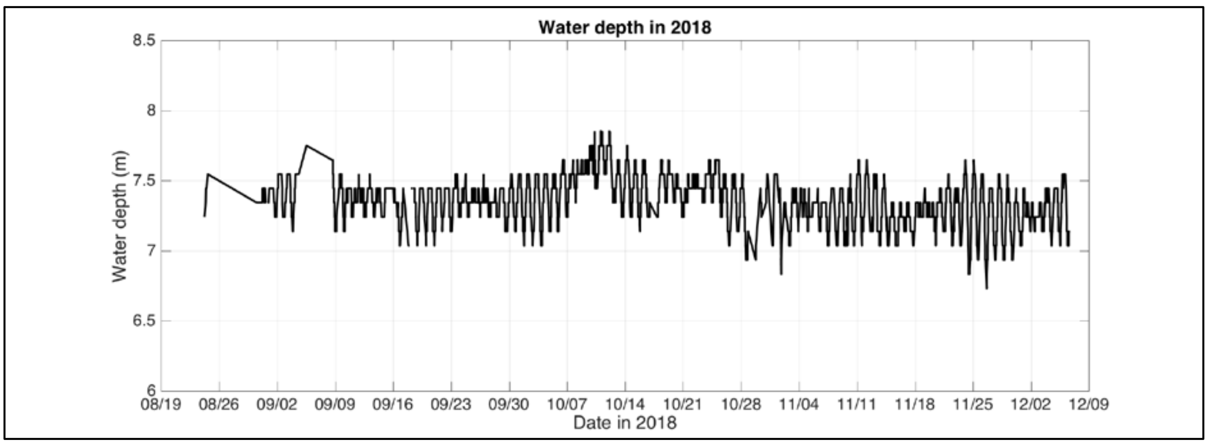

Figure 3.4. Time series of water depth above the ADCP before December 6, 2018.

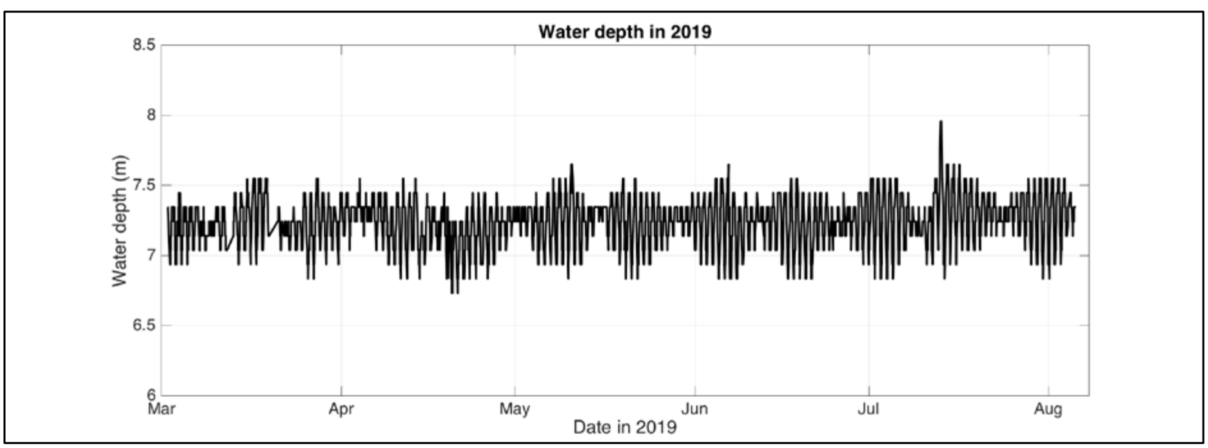

Figure 3.5. Time series of water depth above the ADCP after March 2, 2019.

Water Level. The time series for the water level variations or the water depth variation above the pressure sensor of the acoustic Doppler profiler **(**ADCP) shows daily tidal and fortnightly (two-week) tidal variations (Figures 3.4–3.5). However, the pressure sensor built in the acoustic wave and current sensor (AWAC_ ADCP does not have very high resolution for water level. This is not a major problem because the pressure on the ADCP here serves mainly to indicate where the surface is when the velocity time series is measured. The vertical bins of the horizontal velocity components, however, have a resolution of 1 m and so anything finer than 1 m does not increase the resolution of the position of the vertical bins.

Water Temperature at ~7 m below Surface. The water temperature was measured at the position of the AWAC ADCP unit, roughly ~7 m below the surface. It can be seen that during the first time period (August 23 and December 6, 2018) the water temperature was overall decreasing (Figure 3.6); during the second time period (March 2–August 6, 2019) the water temperature was overall increasing (Figure 3.7). These are obviously due to the seasonal variations.

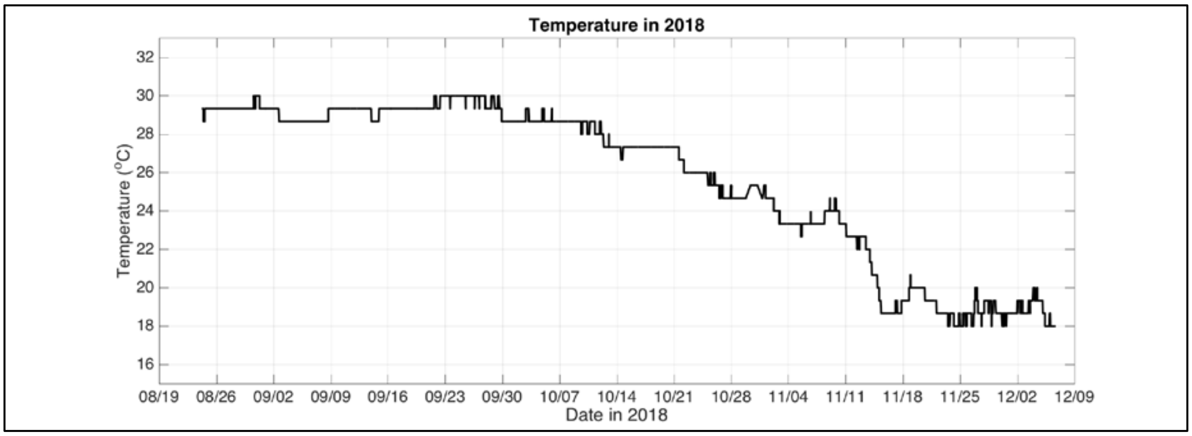

Figure 3.6. Time series of water temperature at the AWAC ADCP unit before December 6, 2018.

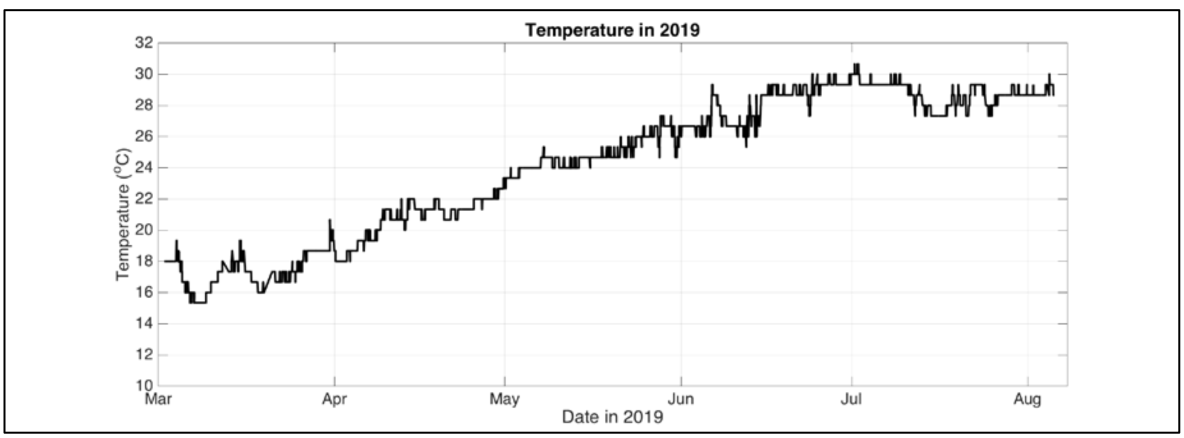

Figure 3.7. Time series of water temperature at the AWAC ADCP unit after March 2, 2019.

Heading and Tilt of the AWAC ADCP. The heading and tilt of the AWAC ADCP showed no variation over the entire period, indicating that the unit was securely mounted and there was no movement during the entire period (Figures 3.8-3.11), even during Hurricane Barry, which passed the area around July 21, 2019.

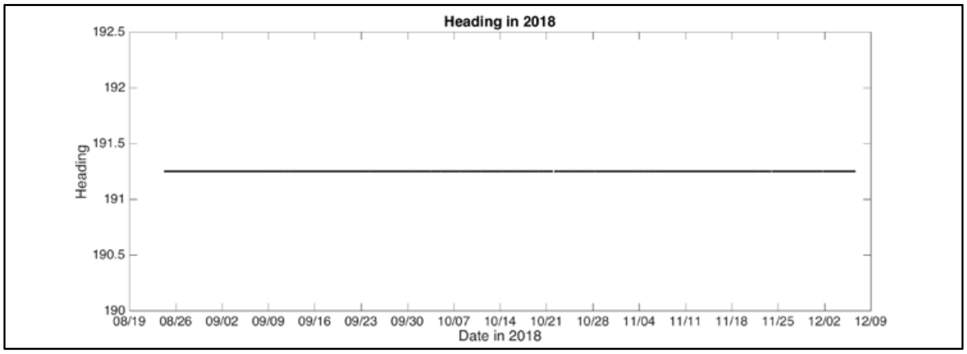

Figure 3.8. Time series of heading of the AWAC ADCP unit before December 6, 2018.

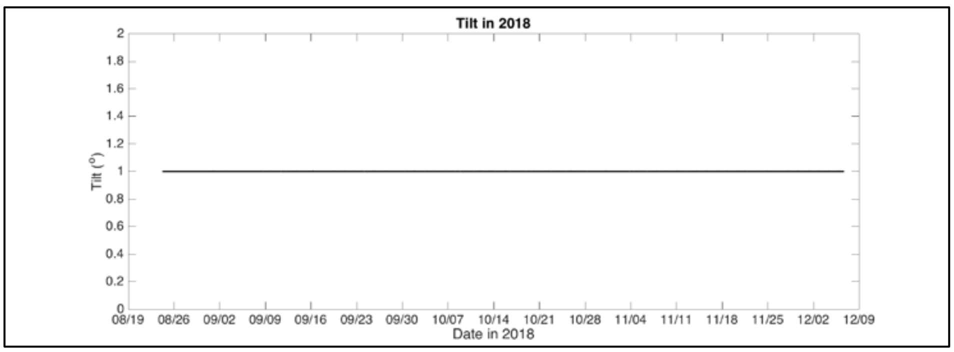

Figure 3.9. Time series of tilt of the AWAC ADCP unit before December 6, 2018.

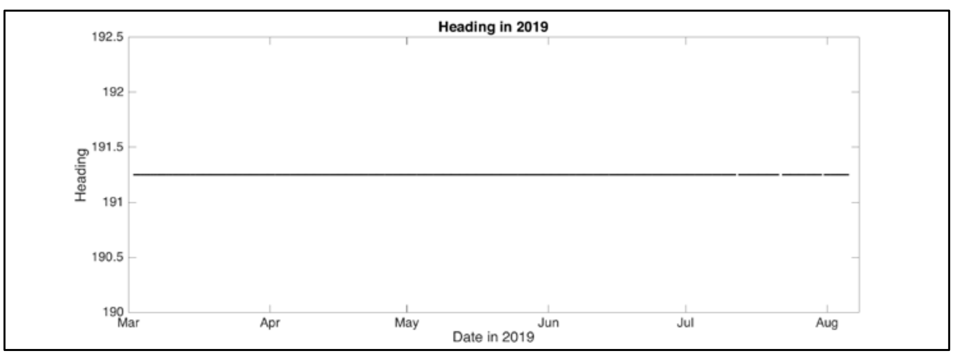

Figure 3.10. Time series of heading of the AWAC ADCP unit after March 2, 2019.

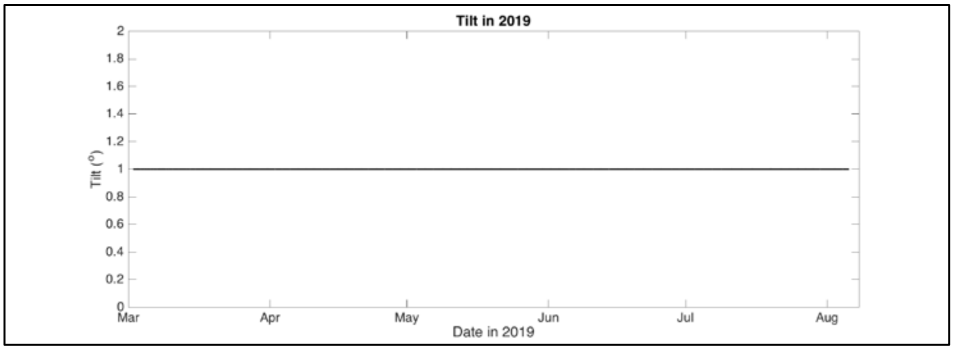

Figure 3.11. Time series of tilt of the AWAC ADCP unit after March 2, 2019.

Flow Direction, Magnitude, and Vector Components. The horizontal flow velocity was recorded as direction and magnitude at 1 m intervals in the vertical. For the first time period (August 23–December 6, 2018), the time series of the flow direction is shown in Figures 3.12–3.19; the time series of the flow magnitude is shown in Figures 3.20–3.27. The decomposed east and north velocity components at various depth above the ADCP are shown in Figures 3.28 and3.29.

For the second period (March 2–August 6, 2019), the time series of the flow direction are shown in Figures 3.30–3.37; the time series of the flow magnitude are shown in Figures 3.38–3.45. The decomposed east and north velocity components at various depths above the ADCP are shown in Figures 3.46 and 3.47.

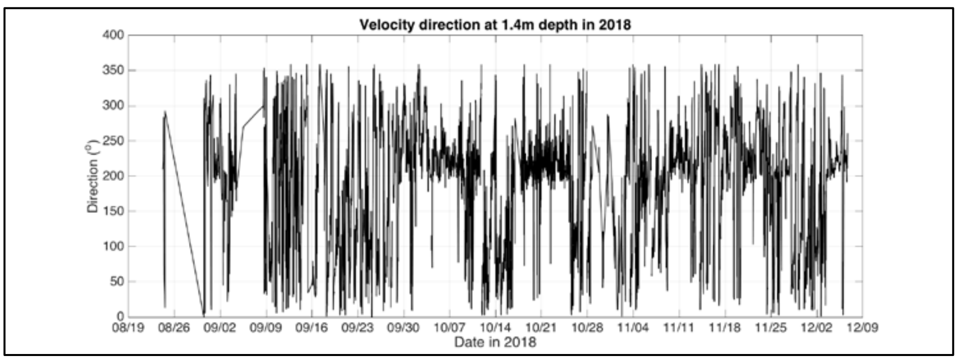

Figure 3.12. Velocity direction at 1.4 m above the ADCP for August 23–December 6, 2018.

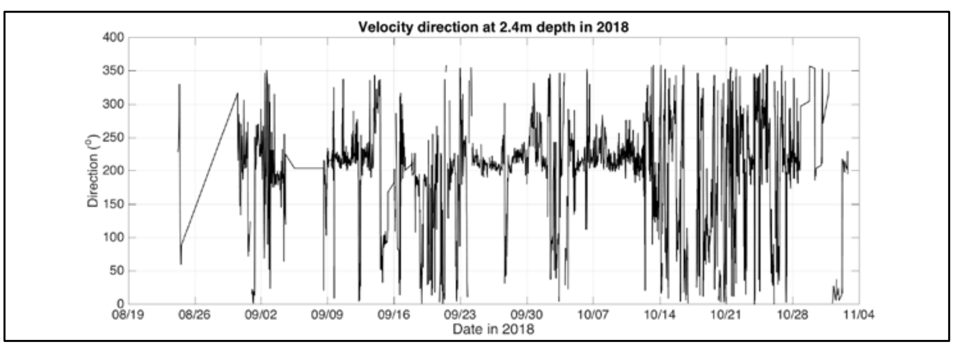

Figure 3.13. Velocity direction at 2.4 m above the ADCP for August 23–December 6, 2018.

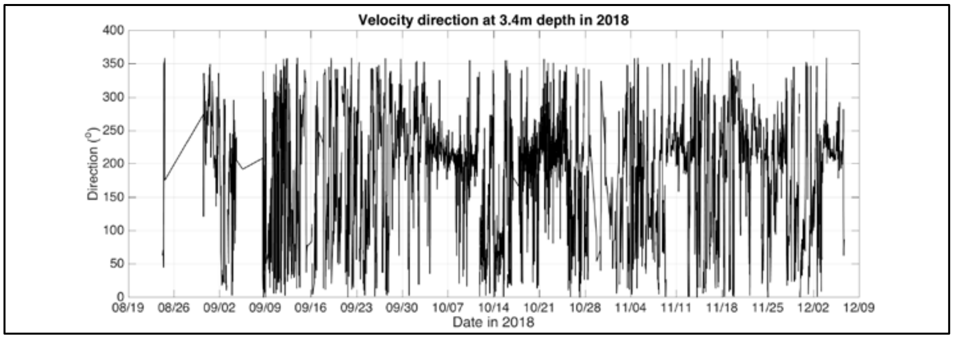

Figure 3.14. Velocity direction at 3.4 m above the ADCP for August 23–December 6, 2018.

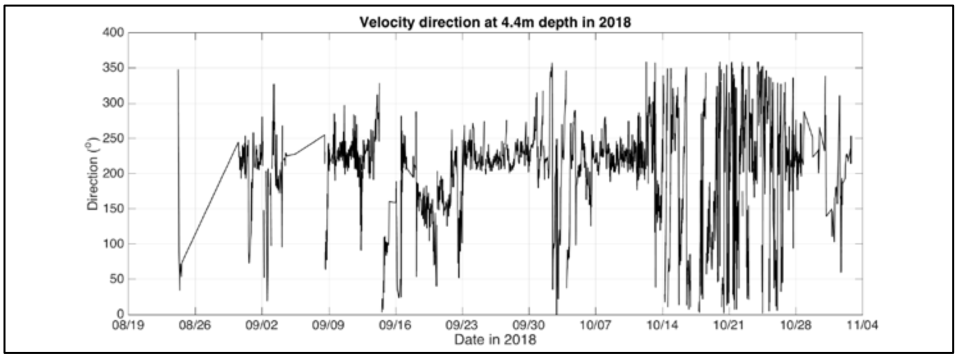

Figure 3.15. Velocity direction at 4.4 m above the ADCP for August 23–December 6, 2018.

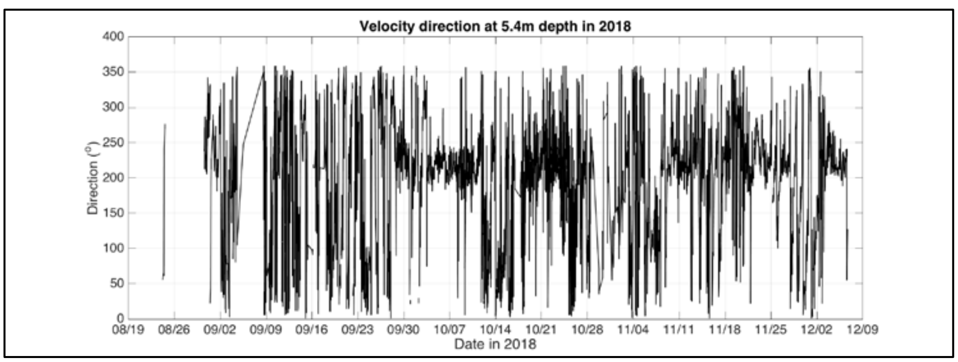

Figure 3.16. Velocity direction at 5.4 m above the ADCP for August 23–December 6, 2018.

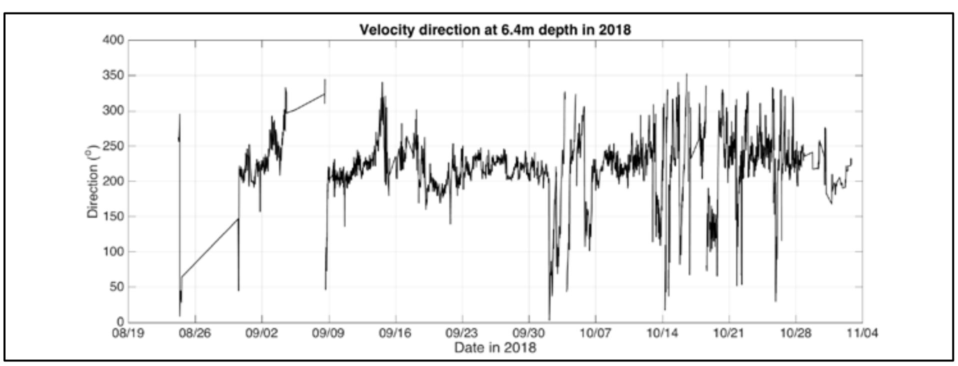

Figure 3.17. Velocity direction at 6.4 m above the ADCP for August 23–December 6, 2018.

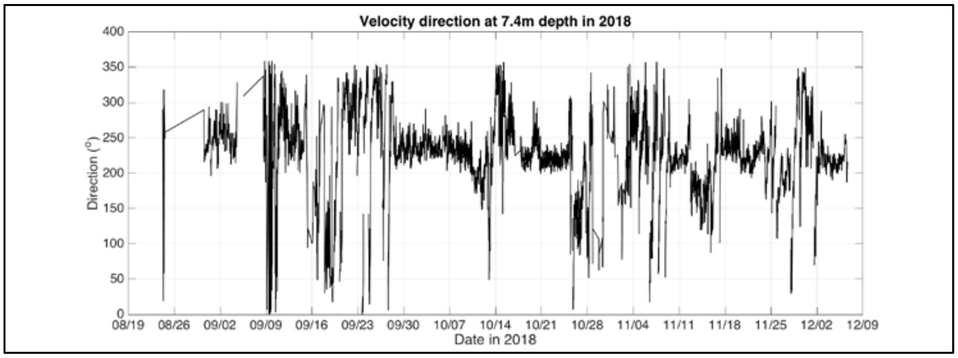

Figure 3.18. Velocity direction at 7.4 m above the ADCP for August 23–December 6, 2018.

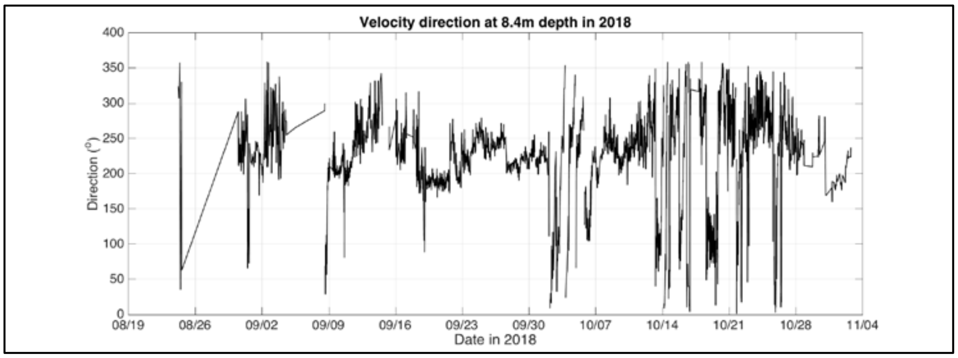

Figure 3.19. Velocity direction at 8.4 m above the ADCP for August 23–December 6, 2018.

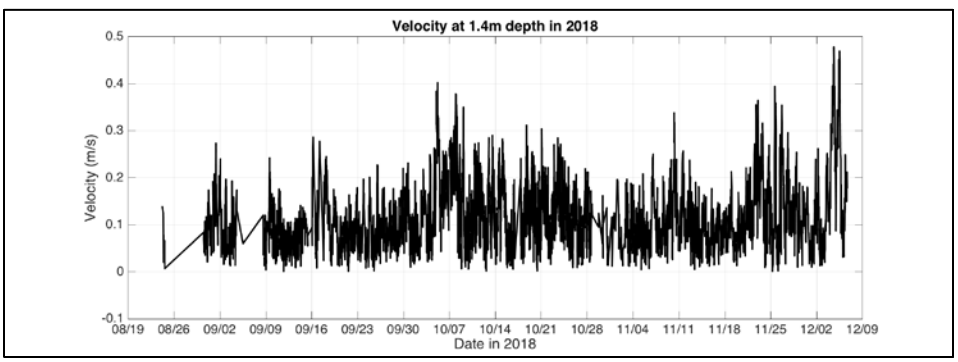

Figure 3.20. Velocity magnitude at 1.4 m above the ADCP for August 23–December 6, 2018.

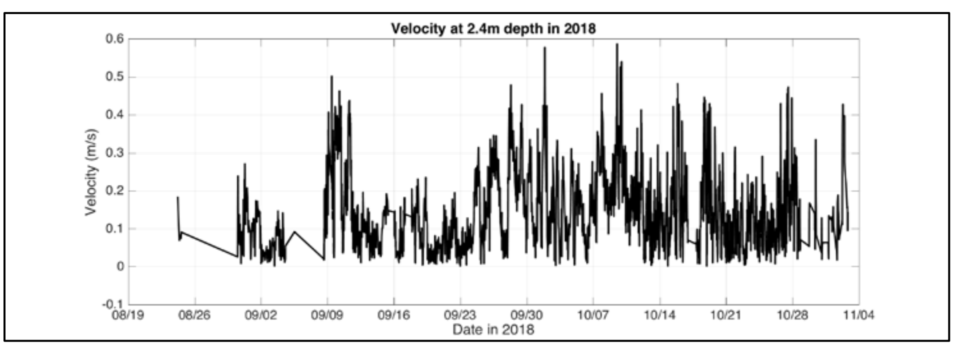

Figure 3.21. Velocity magnitude at 2.4 m above the ADCP for August 23–December 6, 2018.

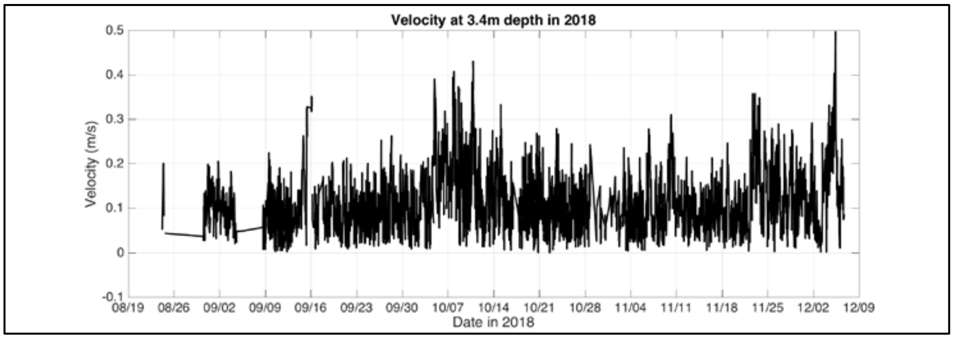

Figure 3.22. Velocity magnitude at 3.4 m above the ADCP for August 23–December 6, 2018.

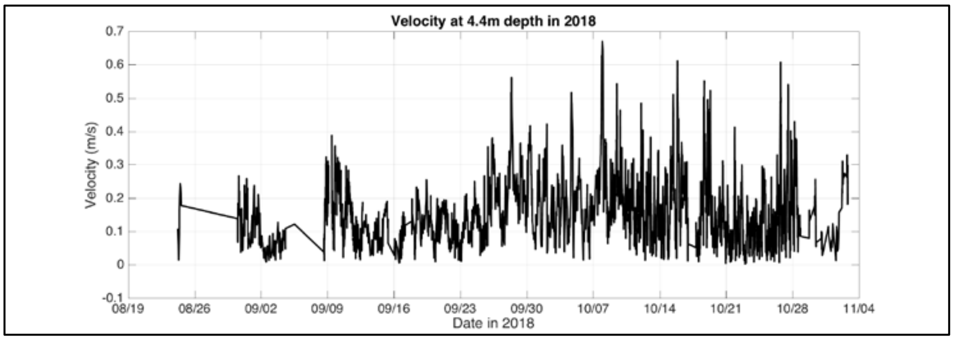

Figure 3.23. Velocity magnitude at 4.4 m above the ADCP for August 23–December 6, 2018.

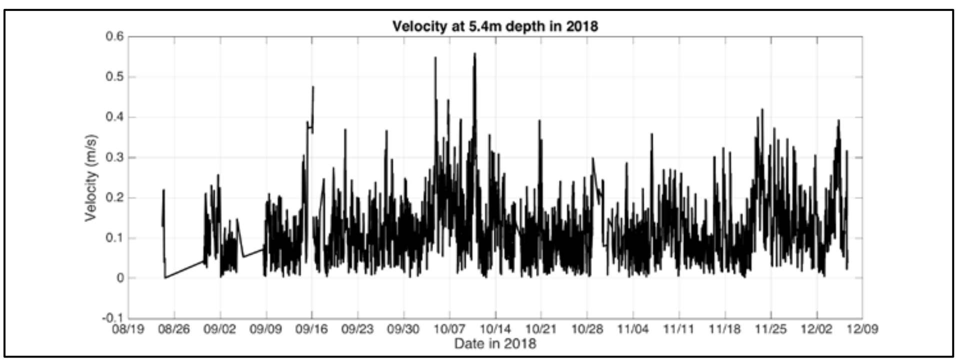

Figure 3.24. Velocity magnitude at 5.4 m above the ADCP for August 23–December 6, 2018.

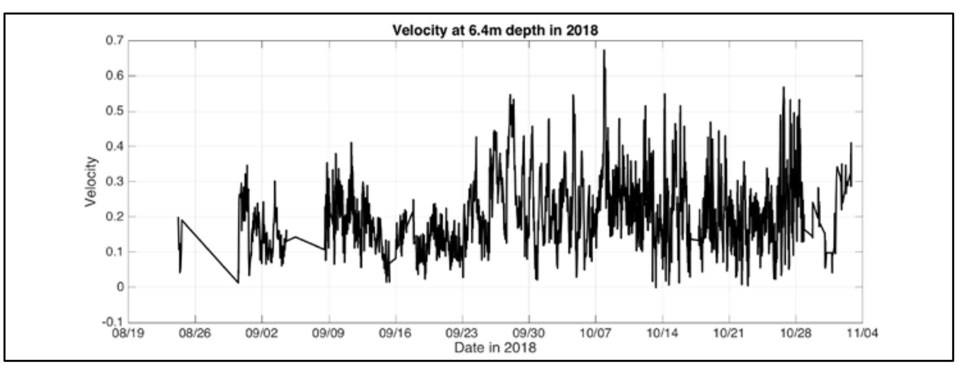

Figure 3.25. Velocity magnitude at 6.4 m above the ADCP for August 23–December 6, 2018.

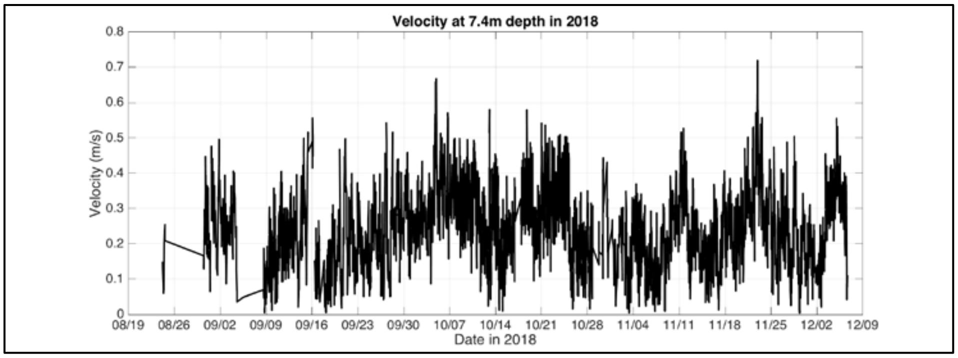

Figure 3.26. Velocity magnitude at 7.4 m above the ADCP for August 23–December 6, 2018.

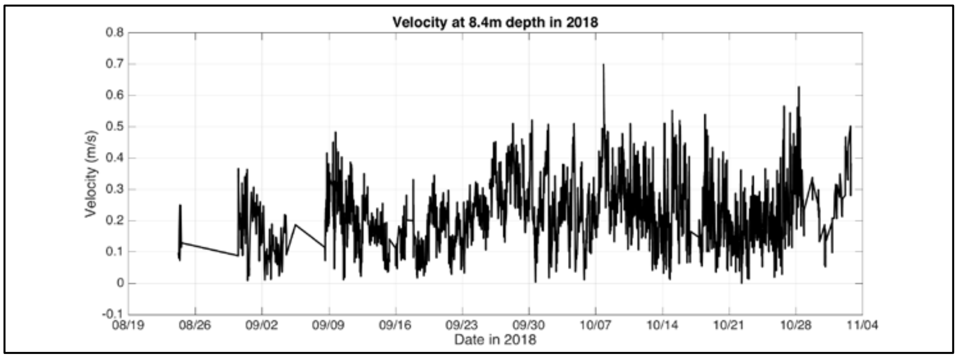

Figure 3.27. Velocity magnitude at 8.4 m above the ADCP for August 23–December 6, 2018.

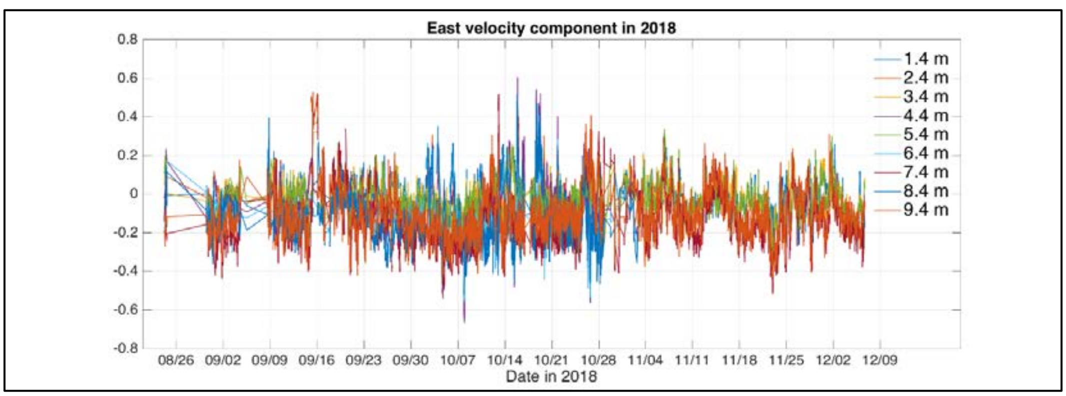

Figure 3.28. East velocity component at various depths above the ADCP for August 23–December 6, 2018.

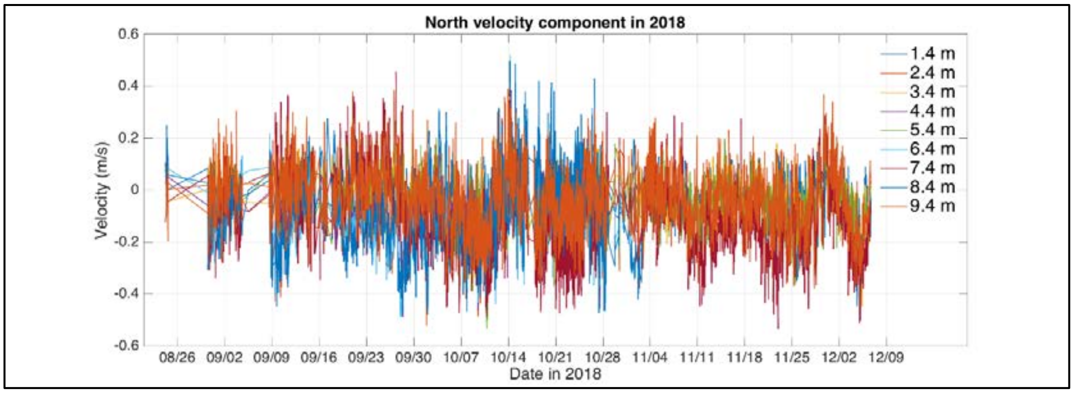

Figure 3.29. North velocity component at various depths above the ADCP for August 23–December 6, 2018.

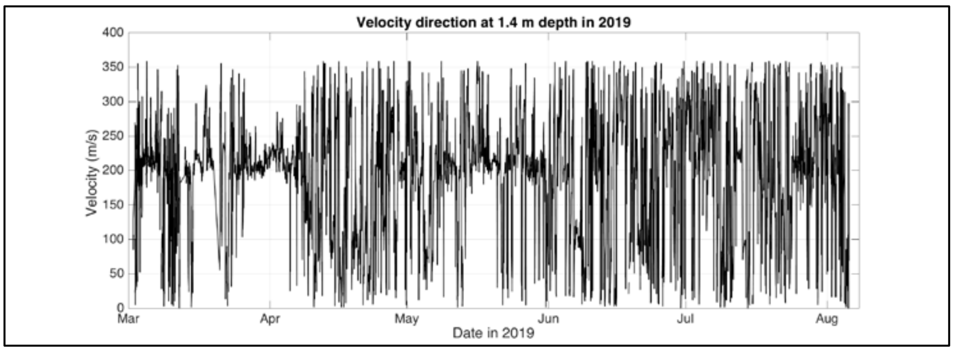

Figure 3.30. Velocity direction at 1.4 m above the ADCP for March 2–August 6, 2019.

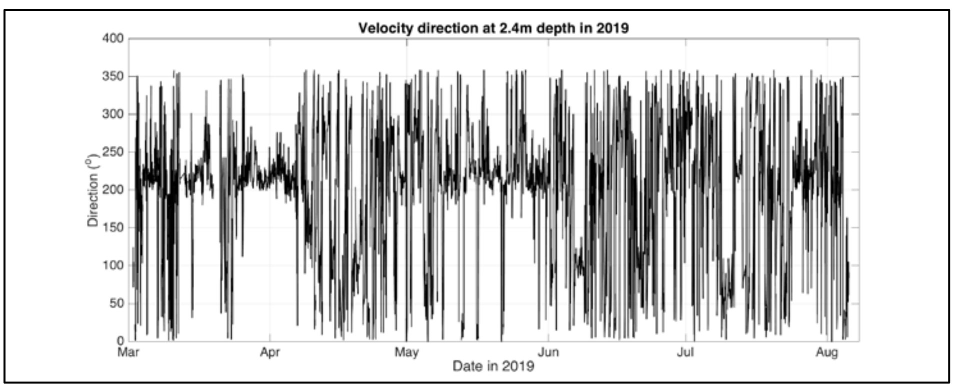

Figure 3.31. Velocity direction at 2.4 m above the ADCP for March 2–August 6, 2019.

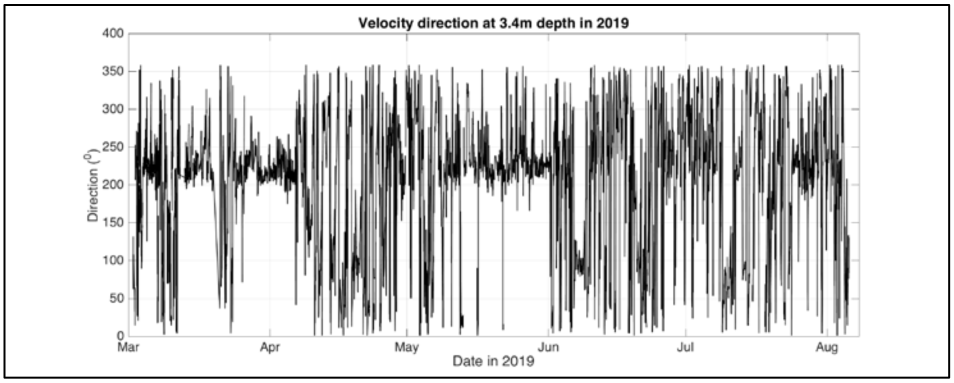

Figure 3.32. Velocity direction at 3.4 m above the ADCP for March 2–August 6, 2019.

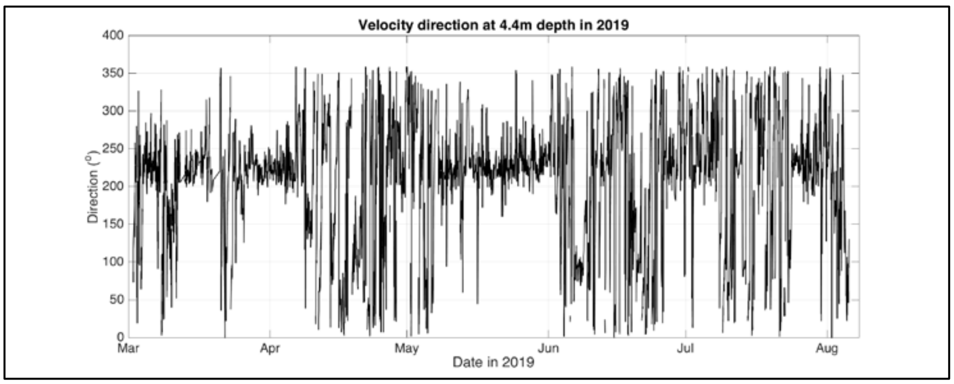

Figure 3.33. Velocity direction at 4.4 m above the ADCP for March 2–August 6, 2019.

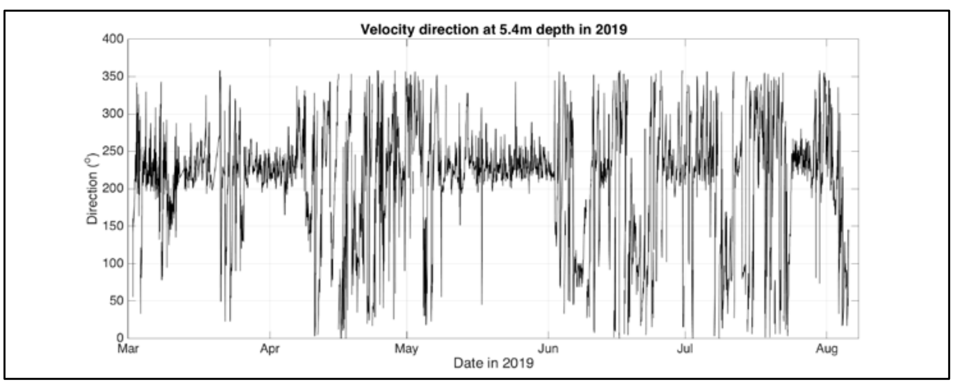

Figure 3.34. Velocity direction at 5.4 m above the ADCP for March 2–August 6, 2019.

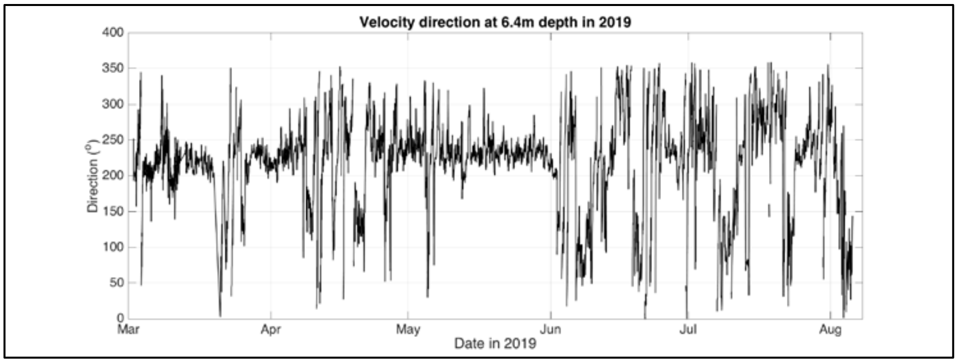

Figure 3.35. Velocity direction at 6.4 m above the ADCP for March 2–August 6, 2019.

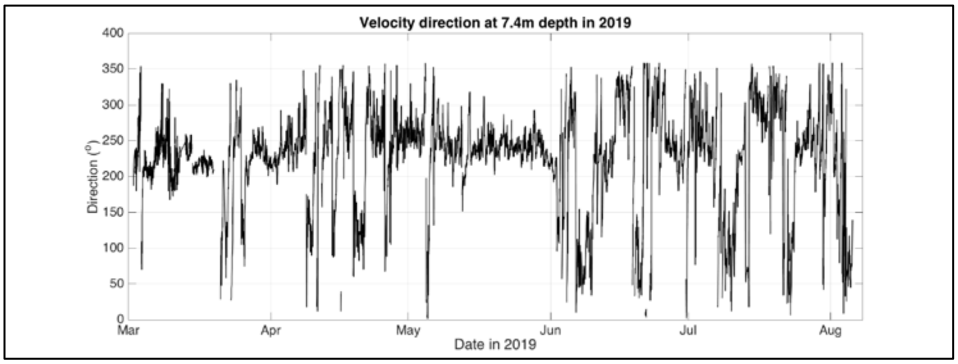

Figure 3.36. Velocity direction at 7.4 m above the ADCP for March 2–August 6, 2019.

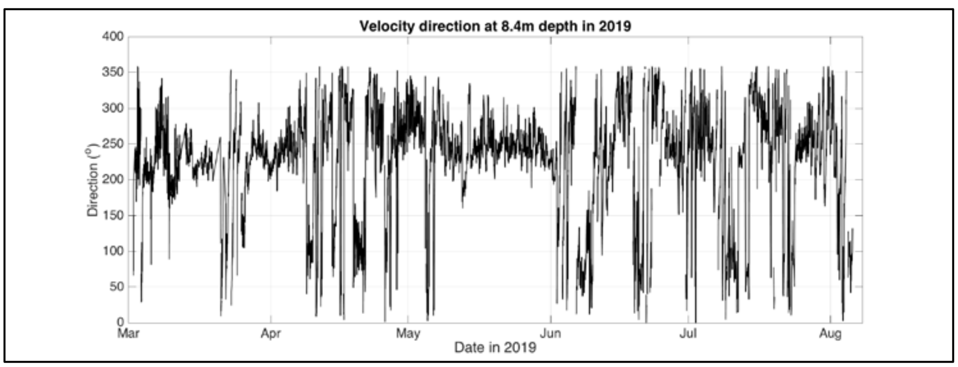

Figure 3.37. Velocity direction at 8.4 m above the ADCP for March 2–August 6, 2019.

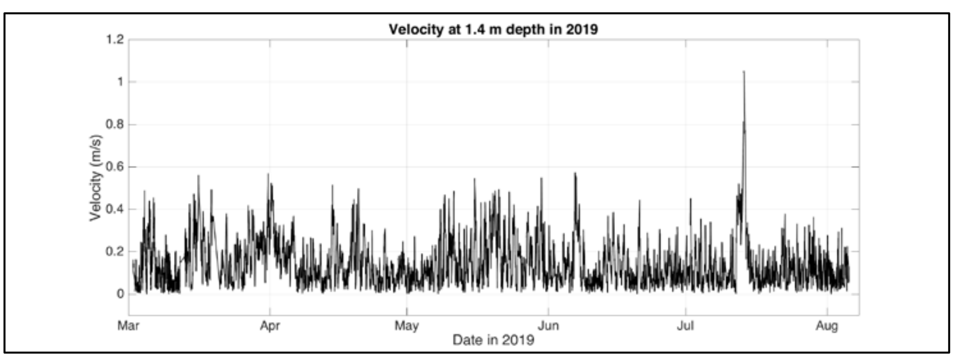

Figure 3.38. Velocity magnitude at 1.4 m above the ADCP for March 2–August 6, 2019.

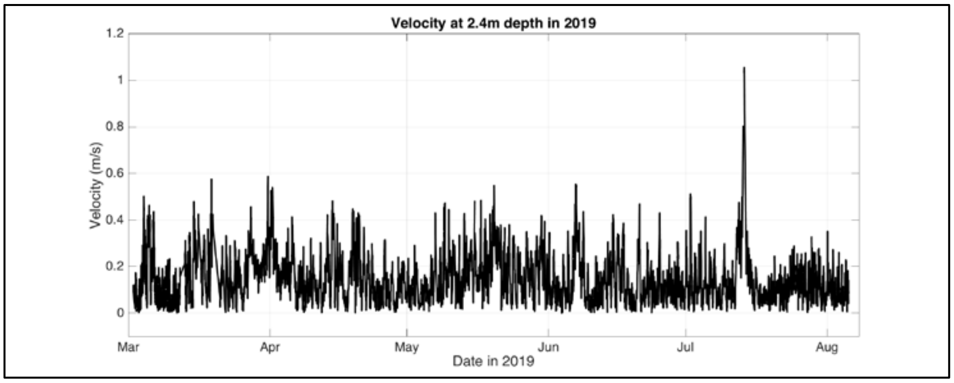

Figure 3.39. Velocity magnitude at 2.4 m above the ADCP for March 2–August 6, 2019.

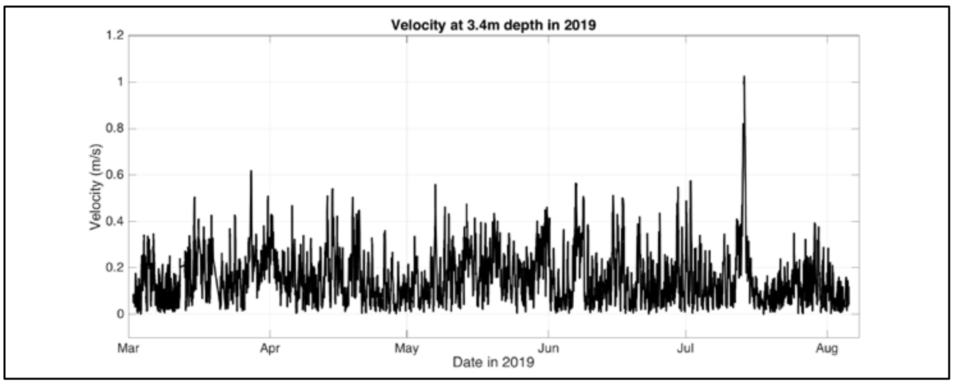

Figure 3.40. Velocity magnitude at 3.4 m above the ADCP for March 2–August 6, 2019.

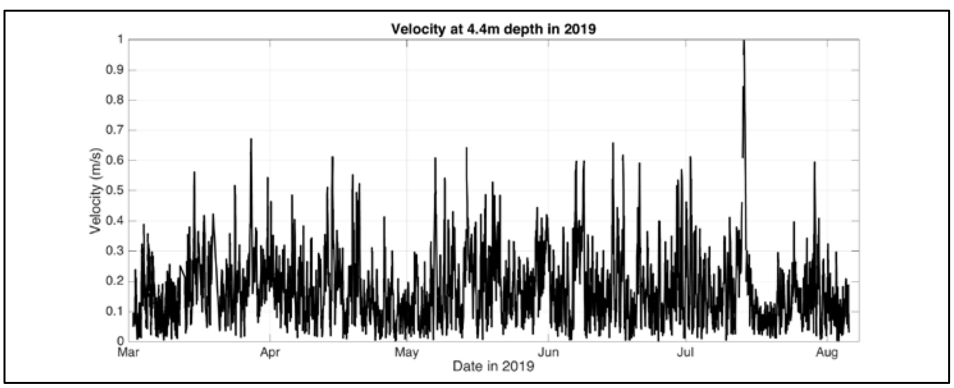

Figure 3.41. Velocity magnitude at 4.4 m above the ADCP for March 2–August 6, 2019.

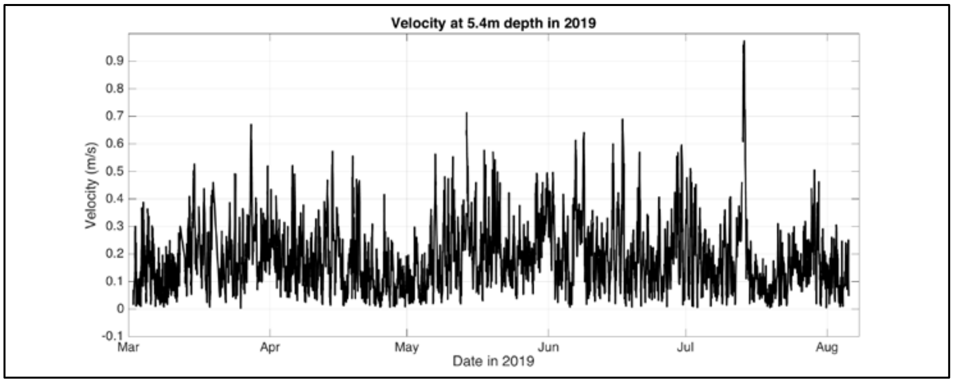

Figure 3.42. Velocity magnitude at 5.4 m above the ADCP for March 2–August 6, 2019.

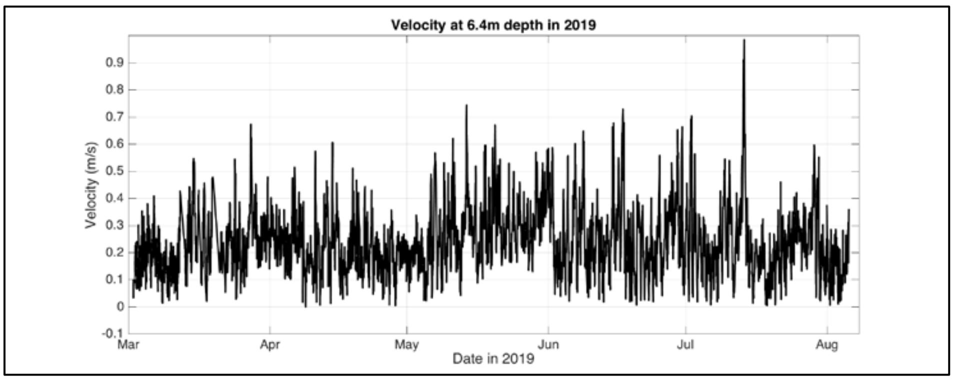

Figure 3.43. Velocity magnitude at 6.4 m above the ADCP for March 2–August 6, 2019.

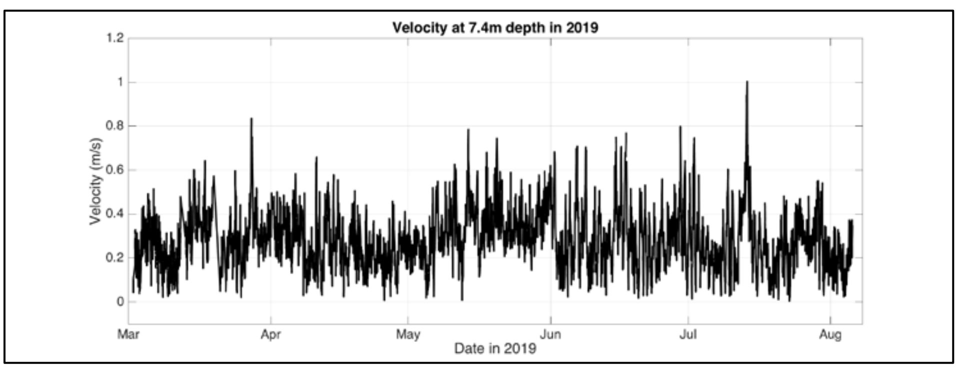

Figure 3.44. Velocity magnitude at 7.4 m above the ADCP for March 2–August 6, 2019.

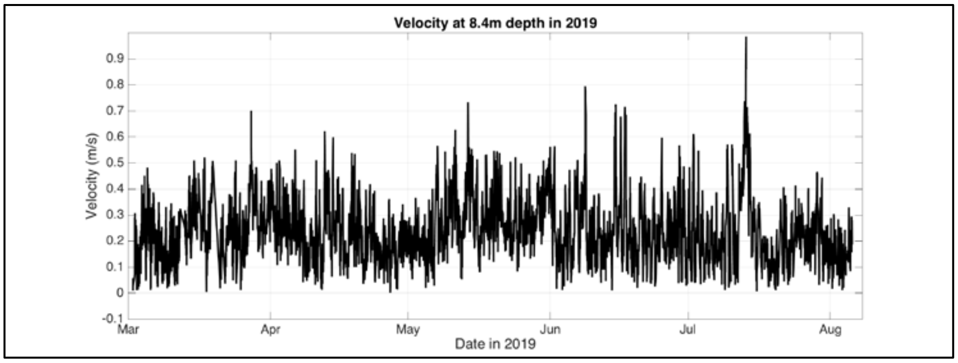

Figure 3.45. Velocity magnitude at 8.4 m above the ADCP for March 2–August 6, 2019.

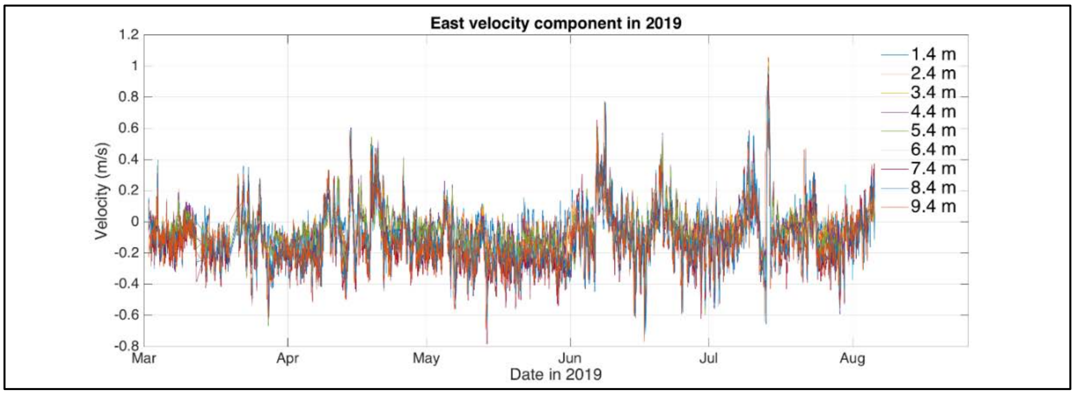

Figure 3.46. East velocity component at various depths above the ADCP for March 2–August 6, 2019.

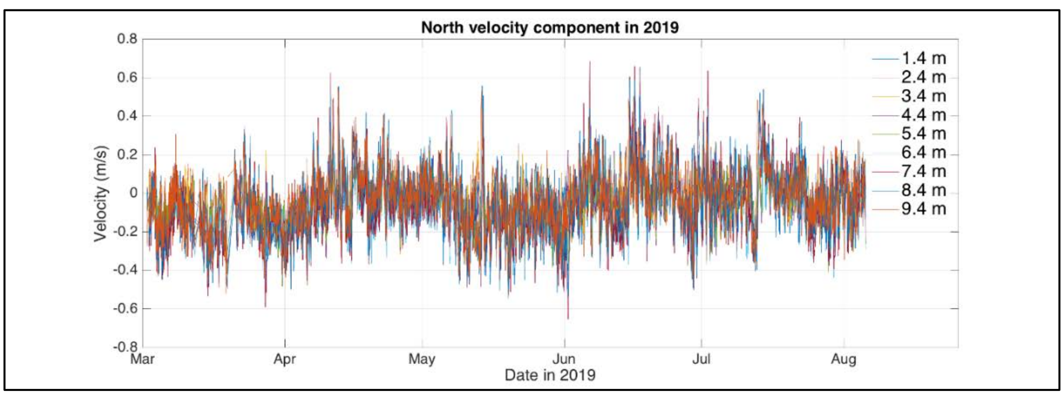

Figure 3.47. North velocity component at various depths above the ADCP for March 2–August 6, 2019.

3.2 The Short-term CTD and Optical Data

The conductivity-temperature-depth sensor (CTD) and ECO-w data are not real time; they are saved in the internal memory of the instrument. There has not yet been a download from these instruments because of difficulties in ship time scheduling and the availability of divers for the retrieval of the equipment. These instruments operate independent of the real time ADCP AOS system and can be redeployed independently in the future.

After retrieving the equipment from its deployment site along the Louisiana coast, we plan to first assess the state of the instrument and attempt to retrieve the data from the instrument memory. The most relevant data is the backscattering time series data. This data will be converted to suspended particulate matter (SPM) based on the pre-deployment calibration measurements. The SPM data will be analyzed in conjunction with physical measurements (currents, waves, weather) to obtain a mechanistic understanding of the variability of suspended material at the study site. We will also examine satellite ocean color data during the sampling period and assess spatial variability of SPM in the study region. The additional measurements of colored dissolved organic matter (CDOM) and chlorophyll fluorescence will contribute to assessing constraints on satellite SPM estimates.

3.3 Weather Conditions during the Deployment

Because the flow conditions in this region are significantly affected by the weather, we compiled the severe weather events during these time periods. The data collected so far cover periods from August 2018–December 9, 2018; and March 3, 2019 (still going). For these periods, we have identified 25 atmospheric events for the 2018 data; and 28 events for the 2019 data (up to August 6). These events include two hurricanes (Hurricane Michael in 2018 and Hurricane Barry in 2019), one tropical storm, 10 stationary fronts, 33 cold fronts, and seven warm fronts. Li et al. (2018) studied the impacts of 76 atmospheric frontal events that include cold, warm, and cold-warm front combinations, and demonstrated that these atmospheric events are important in driving the coastal-estuarine circulations. Likewise, these events should also have significant effects on the hydrodynamics of coastal offshore inner shelf region. Given the unique data we obtain from this region, including those from our new station at SS91, the events identified in Tables 3.1–3.2 can be the subjects of future study for the impact to the circulation and sediment transport. For instance, as subjects of study, we have selected Tropical Storm Gordon (Figures 3.48–3.50), a typical stationary front (Figure 3.51), Hurricane Michael (Figures 3.52–3.54) in 2018, and a cold front (Figure 3.55), a warm front (Figure 3.56), and Hurricane Barry (Figures 3.57–3.59) in 2019. We have analyzed the National Oceanic and Atomospheric Administration’s (NOAA’s) reanalysis weather data associated with our oceanographic data. This is ongoing research.

Table 3.1. Atmospheric Frontal Events between September 4 and December 9, 2018

Begin Y	M	D	UTC	End M	D	UTC	Type
2018	**9**	**4**	**15**	**9**	**5**	**12**	**Tropical Storm Gordon**
	9	**10**	**18**	**9**	**12**	**3**	**stationary front**
	9	27	0	9	28	0	cold front
	9	28	3	9	28	21	stationary front
	10	**10**	**3**	**10**	**10**	**21**	**Hurricane Michael**
	10	10	21	10	11	9	cold front
	10	13	6	10	13	15	cold front
	10	15	15	10	16	9	cold front
	10	20	15	10	21	6	cold front
	10	25	6	10	25	15	warm front
	10	25	15	10	26	3	cold front
	11	1	3	11	2	3	cold front
	11	4	12	11	5	0	cold front
	11	6	9	11	6	21	cold front
	11	8	0	11	9	12	stationary front
	11	12	6	11	12	12	warm front
	11	12	15	11	13	6	cold front
	11	18	21	11	20	6	cold front
	11	25	9	11	25	18	warm front
	11	25	18	11	26	6	cold front
	12	1	12	12	2	12	cold front
	12	2	15	12	3	0	cold front
	12	3	0	12	3	12	cold front
	12	7	18	12	8	9	stationary front
	12	9	15	12	9	3	cold front

Table 3.2. Atmospheric Frontal Events between March 2 and August 6, 2019

Begin				**End**			
Y	**M**	**D**	**UTC**	**M**	**D**	**UTC**	
2019	3	2	9	3	2	21	**Type**
2019	3	3	12	3	4	3	stationary front
2019	3	11	9	3	12	21	cold front
2019	3	13	3	3	13	15	cold front
2019	3	14	9	3	15	15	warm front
2019	3	19	3	3	19	18	cold front
2019	3	21	0	3	21	12	cold front
2019	3	25	15	3	26	9	cold front
2019	**3**	**30**	**18**	**3**	**31**	**12**	cold front
2019	**4**	**4**	**12**	**4**	**6**	**3**	**cold front**
2019	4	8	6	4	9	0	**warm front**
2019	4	12	0	4	13	6	cold front
2019	4	14	0	4	14	15	cold front
2019	4	18	12	4	19	12	cold front
2019	4	25	3	4	26	3	cold front
2019	5	4	15	5	5	9	cold front
2019	5	8	0	5	8	9	cold front
2019	5	11	3	5	12	21	stationary front
2019	5	31	21	6	1	6	stationary front
2019	6	3	0	6	3	12	stationary front
2019	6	8	3	6	8	21	stationary front
2019	6	9	6	6	10	3	cold front
2019	6	10	9	6	11	6	stationary front
2019	6	13	9	6	13	21	cold front
2019	6	14	12	6	14	18	cold front
2019	**7**	**12**	**0**	**7**	**14**	**12**	warm front
2019	7	23	3	7	24	3	**Hurricane Barry**
2019	7	26	21	7	27	3	cold front
							warm front

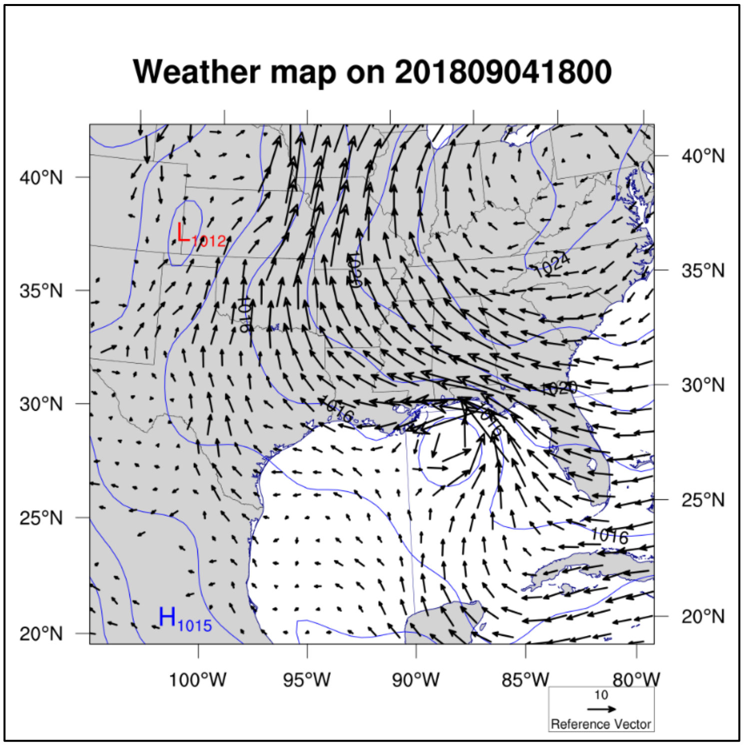

Figure 3.48. Weather map example 1 of 3 for Tropical Storm Gordon.

The vectors are ground level wind velocity–the inset for the reference vector is in m/s. The blue lines are the contours for sea-level air pressure in millibar (mb). The blue letter H and red letter L indicate the high- and low- pressure centers, respectively. These are the same for Figures 3.49–3.59.

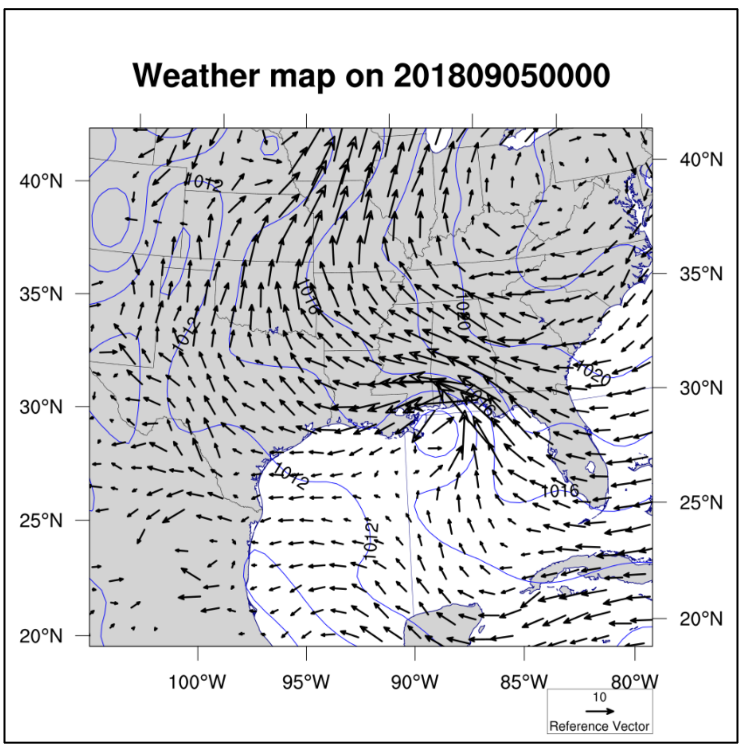

Figure 3.49. Weather map example 2 of 3 for Tropical Storm Gordon.

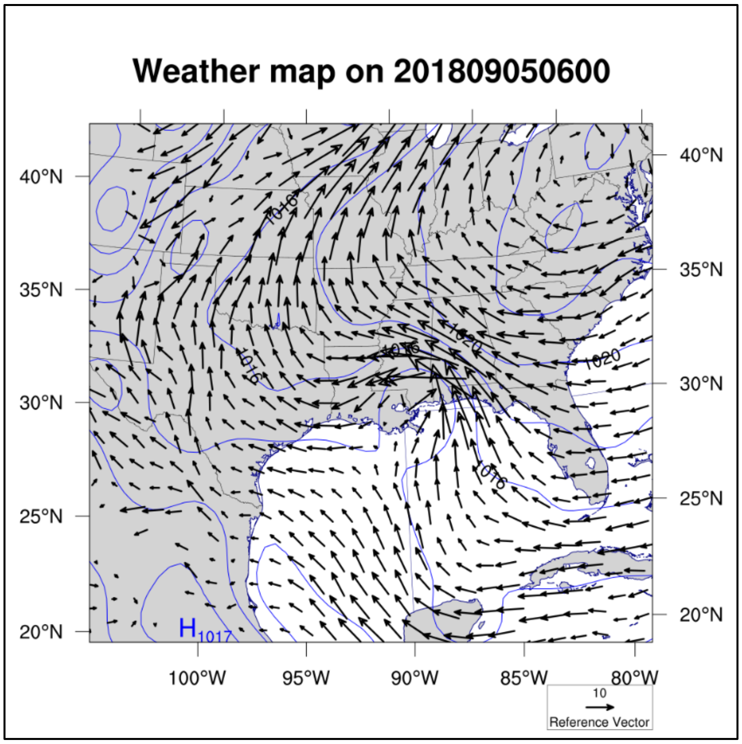

Figure 3.50. Weather map example 3 of 3 for Tropical Storm Gordon.

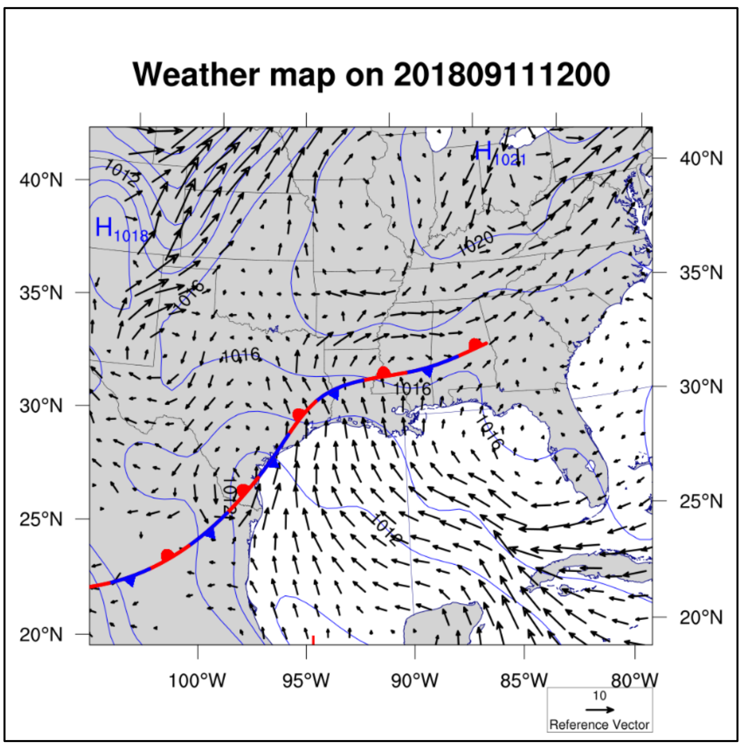

Figure 3.51. Weather map example for a typical stationary front.

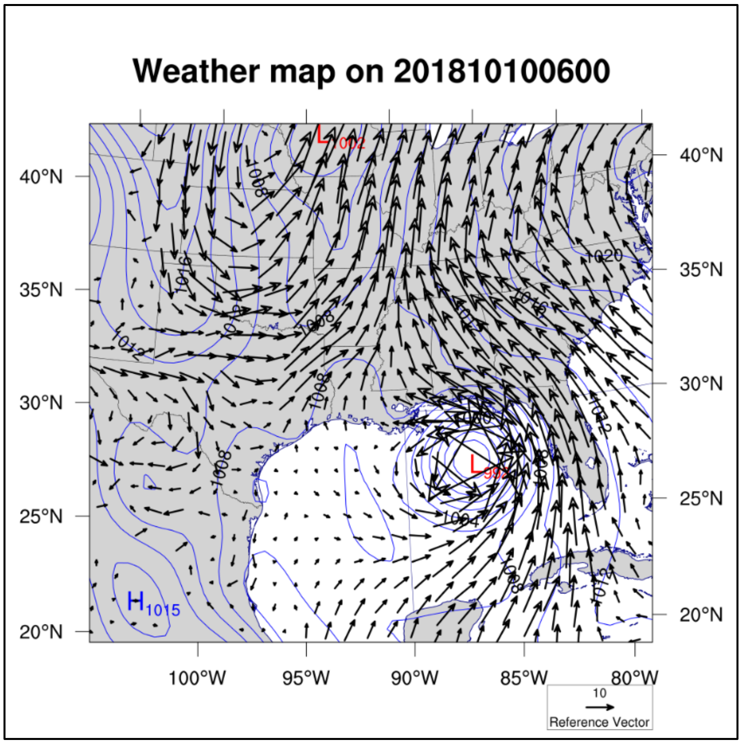

Figure 3.52. Weather map example 1 of 3 for Hurricane Michael.

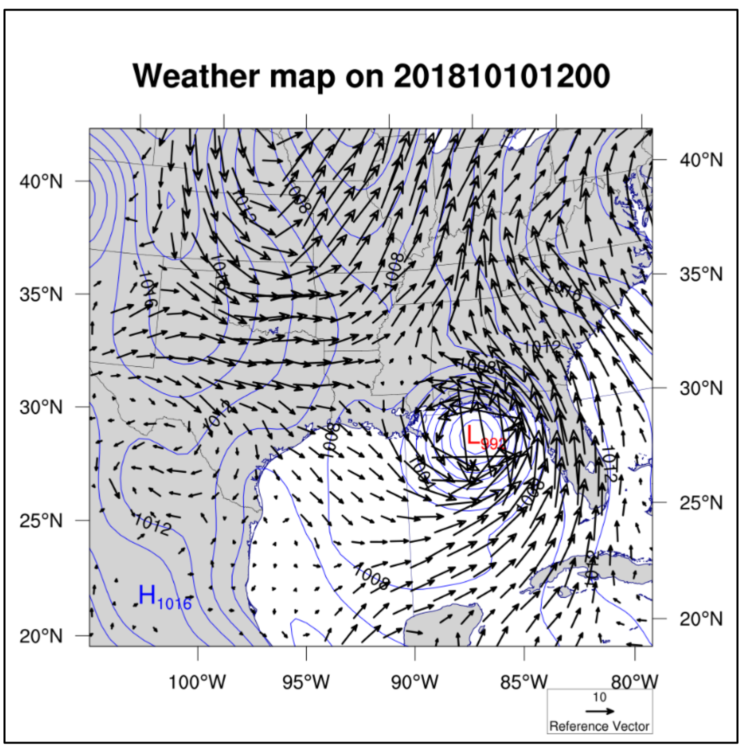

Figure 3.53. Weather map example 2 of 3 for Hurricane Michael.

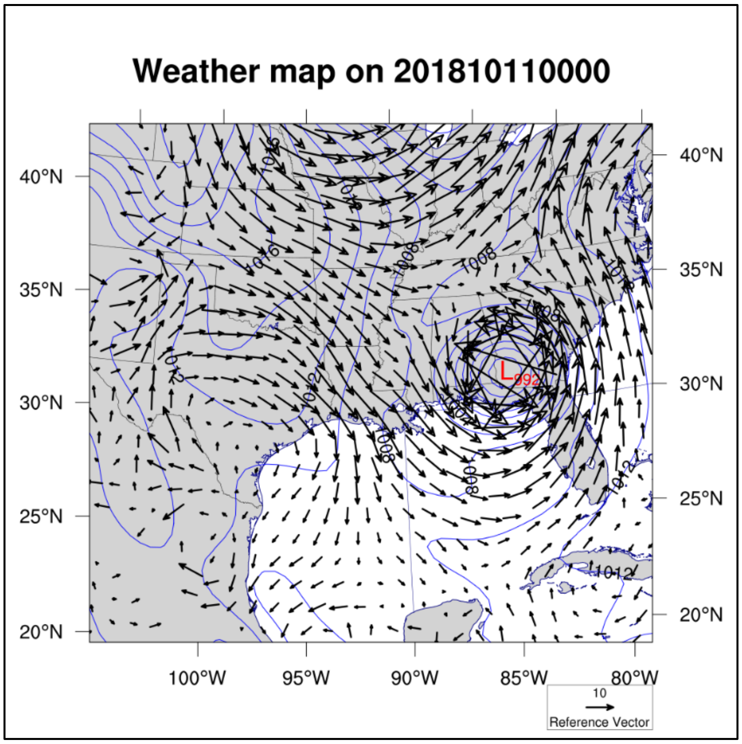

Figure 3.54. Weather map example 3 of 3 for Hurricane Michael.

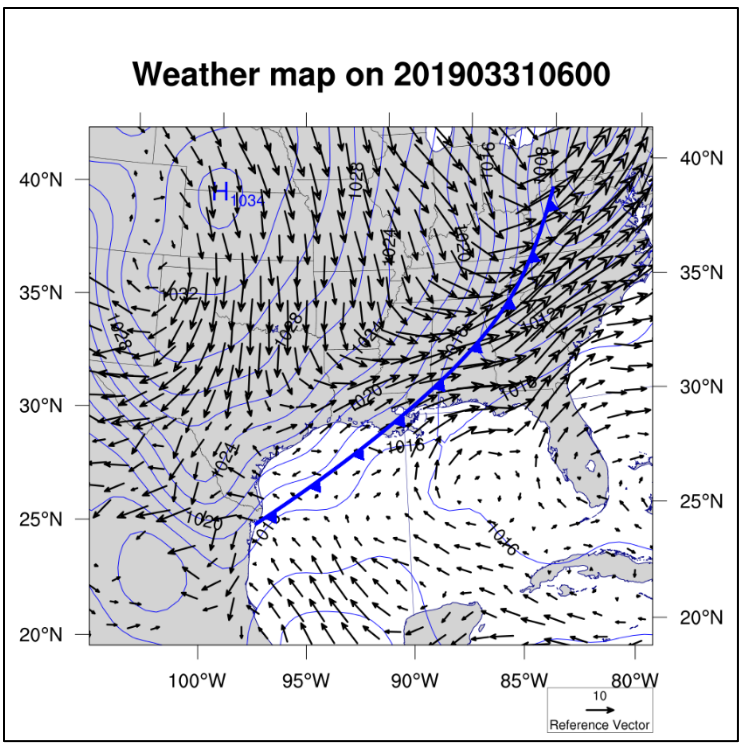

Figure 3.55. Weather map example for a typical cold front.

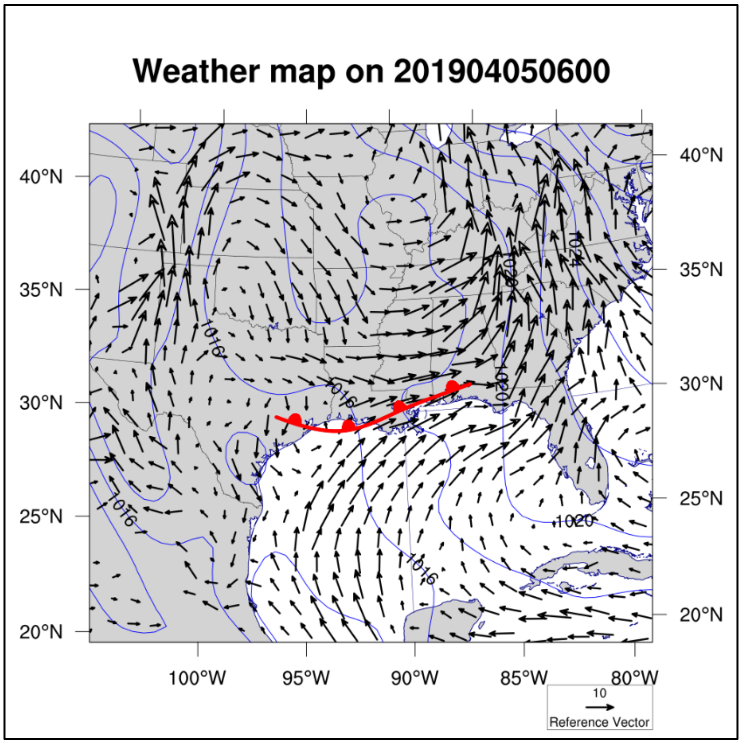

Figure 3.56. Weather map example for a typical warm front.

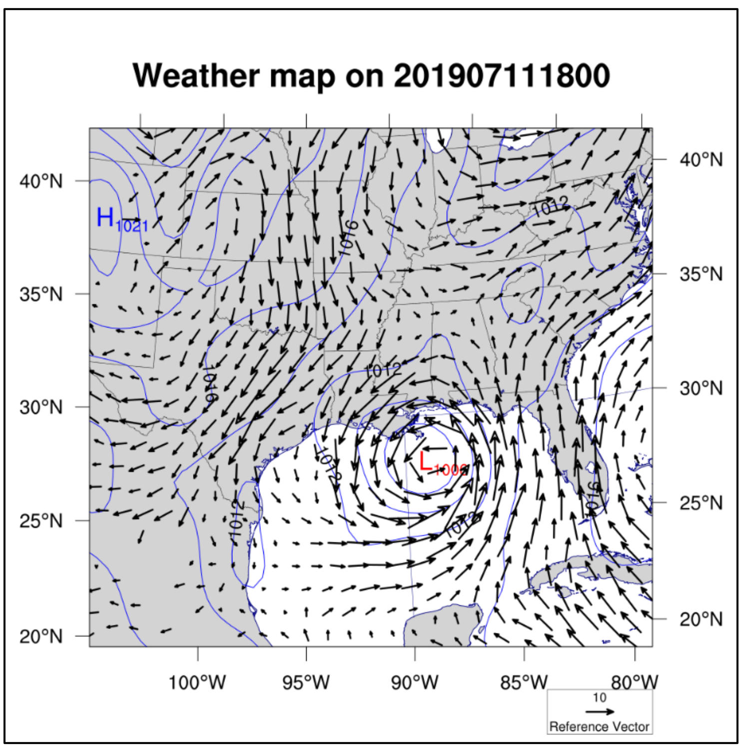

Figure 3.57. Weather map example 1 of 3 for Hurricane Barry.

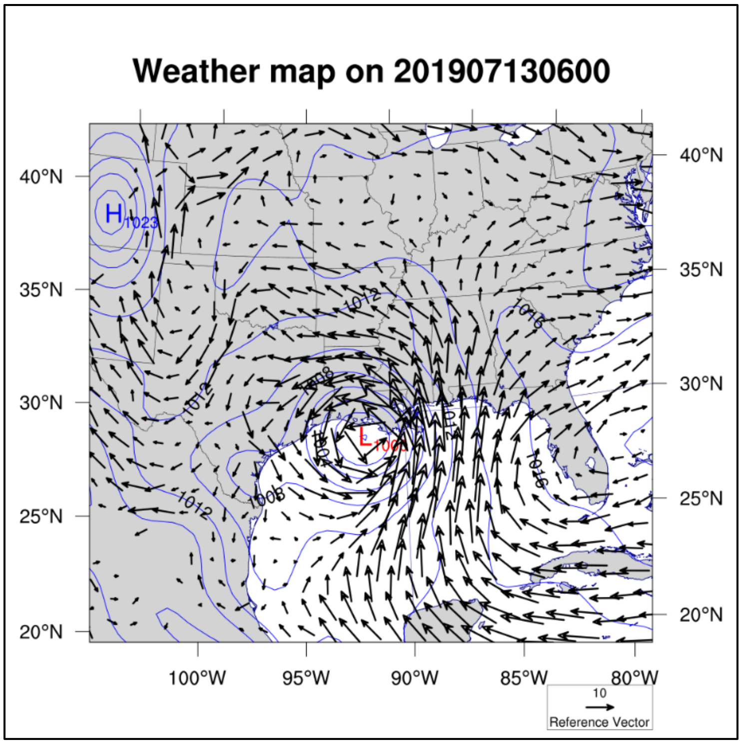

Figure 3.58. Weather map example 2 of 3 for Hurricane Barry.

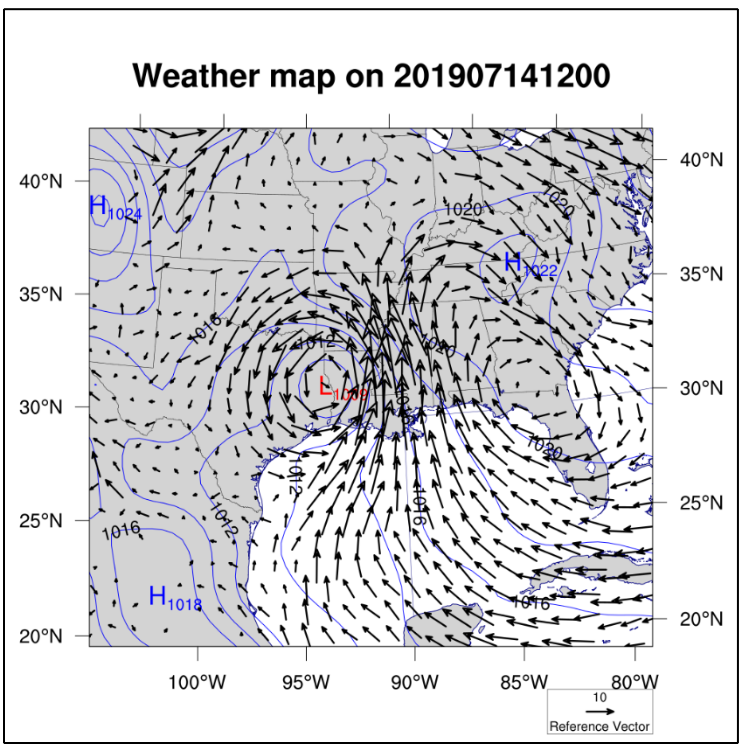

Figure 3.59. Weather map example 3 of 3 for Hurricane Barry.

4. Data Use

The data obtained by the new Wave-Current-Surge Information System (WAVCIS) Station SS91 can be used for many purposes. For example, they can be used to study the hydrodynamic conditions in the area to better understand the sediment transport and evolution of a dredged pit under various tidal and weather conditions, especially under repeated severe weather events, which include the atmospheric cold fronts, warm fronts, combinations of cold-warm fronts (Li et al. 2018), and tropical storms and hurricanes.

4.1 Data Submission

The real time oceanographic data are to be submitted to GCOOS, which is one of the 11 certified regional associations in the US under the Integrated Ocean Observing System (IOOS). GCOOS was created as a member-driven entity in 2005 and incorporated as a nonprofit organization in 2013. In 2018, it was certified by the US Integrated Ocean Observing System and NOAA, indicating that GCOOS is meeting federal standards for data gathering and management and operates inclusively, transparently and seeks user input to determine system priorities. GCOOS is the only regional association of IOOS that covers the entire northern Gulf of Mexico, encompassing the states of Texas, Louisiana, Mississippi, Alabama, and Florida. WAVCIS has been providing QA/QCed data to IOOS/NOAA through GCOOS for almost a decade. The submitted data will be in standard forms that meet all the requirements of NOAA. As a member of GCOOS, WAVCIS has agreed to submit all data from SS91 of this project to GCOOS for broader dissemination and usage.

4.2 Data Usage for Research: Analysis and Numerical Experiments

The data can be used for various research projects. The WAVCIS lab has used the ADCP from the test installation and operation in the Caminada Pass and studied the impact of 51 winter storms to the exchange of water between Barataria Bay and the Louisiana coastal water. More specifically, multiple horizontal ADCPs are used in a long-term deployment to obtain time series data from three inlets of Barataria Bay. One of these ADCPs is a Nortek horizontal profiler using the AOS to transmit the real time data. The data allows an opportunity to study the impact of 51 atmospheric cold fronts to the subtidal exchange flows of the bay with the Louisiana coastal ocean. Analyses demonstrate relations between the weather forcing and subtidal ocean response in the “weather band” (3–7 days in period). The prefrontal, frontal, and post-frontal winds produce alternating flows into, out of, and then back into the bay, forming an asymmetric “M” for low-pass filtered flows. A regression explainable by the dynamical balance shows that cold front-induced flows are the most important component in this region and the flows can be predicted based on wind vector time series. The effect of air pressure is small but correlated with the subtidal currents. A numerical simulation using a validated Finite Volume Community Ocean Model (FVCOM) demonstrates that the wind-driven oscillations within the bay are consistent with the quasi-steady state with little influence of Coriolis for cold front-related wind-driven flows. It is also found that the multiple inlets behave in a way such that the inward transport tends to be through the upwind inlet and the downwind inlet tends to have less inward or even outward transport. Shallow (deep) water tends to have downwind (upwind) flows. Counter-wind flows can develop at bottom. The correlation, energy spectrum, dynamics-based regression of these 51 storms, and numerical modeling all demonstrate that cold fronts produce the major subtidal flows in this micro-tidal system. For a more complete presentation showing the value of the data in supporting research, see Li et al. 2019.

4.3 Data Usage for Research: Model Validation and Subsequent Numerical Experiment

The data can also be used for model validation. There is virtually no other source for real-time continuous measurements of velocity profiles over the Louisiana continental shelf at this moment except the WAVCIS station SS91. The data are useful for model validation for studies on hydrodynamics, sediment transport, storm surges, hypoxia, and oil spill, just to name a few. In our own research, we have also used the SS91 data for model validation and subsequent numerical model experiments in a recent effort to determine the transport and coastal currents during and after hurricanes Harvey, Michael, and Barry. Appendix 1 provides some relevant information on this effort.

4.4 Data Use for Student Projects

The WAVCIS data have been provided to numerous users, including students throughout the country for their projects. For example, the data have been used for student dissertations related to the recent BOEM-supported dredged pit projects. In March 2018, Nazanin Chaichitehrani successfully defended her dissertation “Numerical Experiment of Sediment Dynamics over a Dredged Pit on the Louisiana Shelf” in which she used WAVCIS data for analysis and for model validation. We anticipate more students will use the new SS91 station data for dissertations and theses.

5. Summary

In this BOEM-funded project, we have selected a site at SS91, south of Timbalier Bay for the installation of a real time ocean observing station. The station is at a shallow water of ~37 ft on Ship Shoal, where dredging of sand has been ongoing and where there is a need for proper assessment of the fate of a dredged pit under various weather and oceanographic conditions and the integrated effect over the years. This is a station based on an oil production unit owned by the Fieldwood Energy.

We have successfully installed an upward-looking acoustic Doppler profiler (ADCP) at this station for real-time data transfer through Iridium Satellite Communications with an omnidirectional antenna. This system is much smaller than the old Wave-Current-Surge Information System (WAVCIS) stations, which used an onsite desktop computer that was subject to hacking and frequent unwanted system updates with costly data fees. The hacking and unwanted system updates caused interruptions in operation and costly repairs (ship time and labor costs). The new system does not use an onsite computer; new technology is used and an internal processor and data logger replace the onsite computer. In addition, this system does not need the bulky cooling systems at each of the old stations. The old stations also needed heavy and large directional parabolic antennas.

Our intention is to keep the station running and provide the data to BOEM and Gulf Coastal Ocean Observing System (GCOOS). WAVCIS is part of the GCOOS. The data will be crucial for the modeling of sediment transport and the fate of dredged pit off Louisiana coast to support the mission of BOEM's Marine Minerals Program in the Outer Continental Shelf region. The data will be also provided to the National Oceanic and Atmospheric Administration for archive. They will also be used by researchers, students, including people at Louisiana State University and other institutions for studying the hydrodynamics and for numerical model predictions of the oceanic conditions that affect the fate of sediments and potential impact to any mineral resources.

Works Cited

Boss E, Stramski D, Bergman T, Pegau S, Lewis M. 2005. Why should we measure optical backscattering? Oceanography. 17: 44-49.

Cochrane JD, Kelly FJ. 1986. Low-frequency circulation on the Texas-Louisiana continental shelf. J Geophys Res. 91:10645-10659.

D’Sa EJ, Miller RL, Del Castillo C. 2006. Bio-optical properties and ocean color algorithms for coastal waters influenced by the Mississippi River during a cold front. App Op. 45:7410-7428.

D’Sa EJ, Ko DS. 2008. Short-term influences on suspended particulate matter distribution in the northern Gulf of Mexico: satellite and model observations. Sensors. 8:4249-4264.

D’Sa EJ, Korobkin M, Ko DS. 2011. Effects of Hurricane Ike on the Louisiana-Texas coast from satellite and model data. Remote Sensing Lett. 2:11-19.

D’Sa EJ, Goes JI, Gomes H, Mouw C. 2014. Absorption and fluorescence properties of chromophoric dissolved organic matter of the eastern Bering Sea in the summer with special reference to the influence of a Cold Pool. Biogeosci. 11:3225-3244. doi:10.5194/bg-11-3225-2014

D’Sa EJ, Miller RL, McKee BA. 2007. Suspended particulate matter dynamics in coastal waters from ocean color: Application to the northern Gulf of Mexico. J Geophys Res. 34: L23611.

Falcini F, Khan NS, Macelloni L, Horton BP, Lutken CB, et al. 2012. Linking the historic 2011 Mississippi River flood to coastal wetland sedimentation. Nat Geosci. 5: 803-807.

Feng Z, Li C. 2010. Cold-front-induced flushing of the Louisiana bays. J Mar Syst. 82:252-264.

Hsu SA. 1988. Coastal meteorology. San Diego (CA): Academic Press.

Kolker AS, Li C, Walker ND, Pilley C, Ameen AD, et al. 2014. The impacts of the great Mississippi/Atchafalaya River flood on the oceanography of the Atchafalaya Shelf. Cont Shelf Res. 86: 17-33.

Li C. 2013. Subtidal water flux through a multi-inlet system: observations before and during a cold front event and numerical experiments. JGR Oceans. 118(4):1–16. doi:10.1029/2012JC008109

Li C, Weeks E, Blanchard BW. 2010. Storm surge induced flux through multiple tidal passes of Lake Pontchartrain estuary during Hurricanes Gustav and Ike. Estuar Coast Shelf Sci. 87:517–525.

Li C, Weeks E, Milan B, Huang W, Wu R. 2018. Weather induced transport through a tidal channel calibrated by an unmanned boat. J Atmos Oceanic Tech. 35(2): 261-279.

Li C, Weeks E, Rego J. 2009a. In situ measurements of saltwater flux through tidal passes of Lake Pontchartrain Estuary by Hurricanes Gustav and Ike in September 2008. Geophys Res Lett. 36:L19609. doi:10.1029/2009GL039802

Li C, Roberts H, Stone GW, Weeks E, Luo Y. 2011a. Wind surge and saltwater intrusion in Atchafalaya Bay during onshore winds prior to cold front passage. Hydrobiologia. 658(1):27-39. doi:http://dx.doi.org/10.1007/s10750-010-0467-5

Li C, White JR, Chen C, Lin H, Weeks E, et al. 2011b. Summertime tidal flushing of Barataria Bay: transports of water and suspended sediments. J Geophys Res C: Oceans. 116:C04009. DOI:10.1029/2010JC006566

Li C, Walker N, Hou A, Georgiou I, Roberts H, et al. 2008b. Circular plumes in Lake Pontchartrain Estuary under wind straining. Estuar Coast Shelf Sci. 80:161-172.

Li C, Chen C. 2014. Shelf circulation prior to and post a cold front event measured from vessel based acoustic Doppler current profiler. J Marin Sys. 139:38-50.

Li C, Huang W, Milan B. 2019. Atmospheric cold front induced exchange flows through a microtidal multi-inlet bay: analysis using multiple horizontal ADCPs and FVCOM simulations. J Atmos Oceanic Technol. 36:443-472.

Lin J, Li C, Boswell KM, Kimball M, Rozas L. 2016. Examination of winter circulation in a Northern Gulf of Mexico estuary. Estuar Coasts. 39(4): 879-899. doi:http://dx.doi.org/10.1007/s12237-015-0048-y

Nittrouer JA, Allison MA, Campanella R. 2008. Bedform transport rates for the lowermost Mississippi River. J Geogr Res. 113: F03004.

Penland S, Suter JR, MacBride RA, Williams SJ, Kindinger JL, et al. 1989. Holocen sand shoals offshore of the Mississippi River delta plain. GCAGS [Gulf Coast Association of Geologic Societies] Trans. 39:471-480.

Rego J, Li C. 2010a. Storm surge propagation in Galveston Bay during Hurricane Ike. J Marin Syst. 82:265-279.

Rego JL, Li C. 2010b. Nonlinear terms in storm surge predictions: effect of tide and shelf geometry with case study from Hurricane Rita. J Geophys Res C: Oceans. 115: C06020. doi: 10.1029 / 2009JC005285

Roberts HH, Huh OK, Hsu SA, Rouse Jr LJ, Rickman D. 1989. Winter storm impacts on the Chenier Plain Coast of Southwestern Louisiana. Gulf Coast Assoc Geol Soc Trans. 39:(515-522).

Stone GW, Condrey RE, Fleeger JW, Khalil SM. 2009. Environmental investigation of the long-term use of Ship Shoal sand resources for large-scale beach and coastal restoration in Louisiana. 278 p. New Orleans (LA): US Department of Interior, Minerals Management Service, Gulf of Mexico Region. Report No.: OCS Study MMS 2009-024. MMS Contract 1435-01-04-CA-35162 and LCPRA Contract 2503-07-10.

Suter JR, Berryhill Jr HL, Penland S. 1987. Late Quaternary sea-level fluctuations and depositional sequences, southwest Louisiana continental shelf. In: Nummedal D, Pilkey OH, Howard JD, editors. Sea-level fluctuation and coastal evolution. Soc Econ Paleon Mineralog. SEPM Special Publication 41. Tulsa (OK): SEPM [Society of Economic Paleontologists and Mineralogists]. p. 199-219.

Walker ND, Hammack AB. 2000. Impacts of winter storms on circulation and sediment transport: Atchafalaya-Vermilion Bay region, Louisiana, U.S.A. J Coastal Res. 16(4):996-1010.

Zawada DG, Hu C, Clayton T, Chen Z, Brock JC, et al. 2007. Remote sensing of particle backscattering in Chesapeake Bay: a 6-year SeaWiFS retrospective view. Estuar Coast Shelf Sci. 73:792-806.

Zu KH, Bentley SJ, Li C, Chaichitehrani N, Obelcz J, O’Connor M, et al. 2019. An assessment of mud-capped dredge pit evoluation on the outer continental shelf of the Gulf of Mexico. 91 p. New Orleans (LA): US Dept. of the Interior, Bureau of Ocean Energy Management, Gulf of Mexico OCS Region. Contract No.: GM-14-03-05. [in press]

Appendix 1. Numerical Modeling for the Louisiana Continental Shelf

A few models based on the Finite Volume Community Ocean Model (FVCOM) have been developed at Wave-Current-Surge Information System (WAVCIS) with the SS91 acoustic Doppler profiler (ADCP) data for comparison and model validation. Here we use one of them as an example demonstrating the value of data from SS91. The purpose of the model was to simulate the storm current over the shelf for Hurricane Harvey and other severe weather.

Model mesh. The model mesh covers the whole area of the Gulf of Mexico, from 80.7°W to 97.9°W, and 18.1°N to 30.7°N. There are two open boundaries. One is located at the edge of Caribbean Sea, connecting the east border of Mexico and the west edge of Cuba. The other open boundary is located at the North Atlantic Ocean with the northern point at the edge of Florida and the southern point at the border of Cuba. The mesh contains 122664 nodes and 220493 cells (Figures A-1–A-2). The finest resolution is about 20m. There are 40 sigma layers. Time step for the external mode is 1 second. The ratio of the internal time step to external time step is set to be 5.

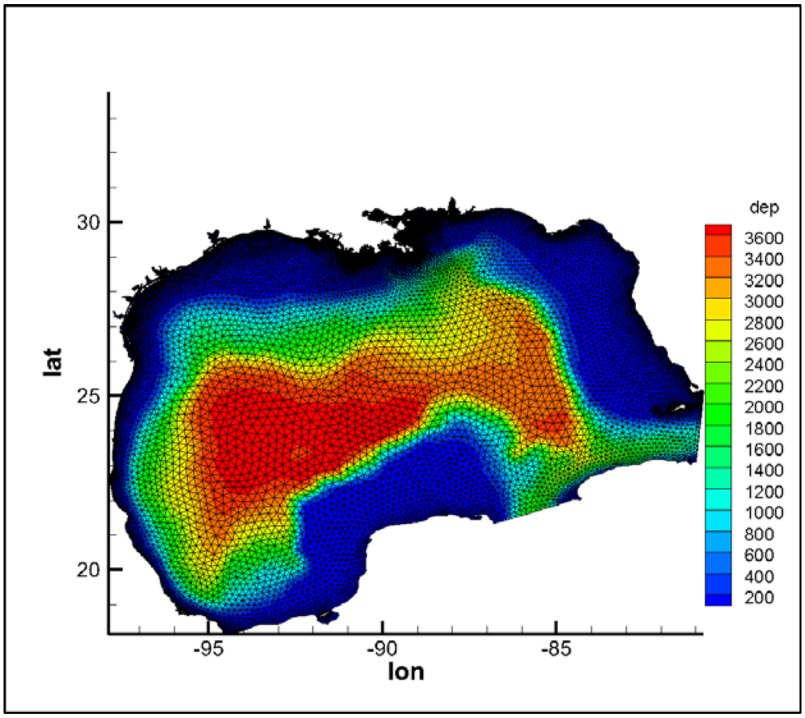

Figure A-1. Model grid for FVCOM.

Experimental design. Time period of numerical simulation is from July 20, 2017 to September 15, 2017. The time interval for the output is 30 minutes. The tide is forced at the open boundary with spatially variable wind and air pressure forcing for the whole area. Tidal forcing is the combination of 10 tidal constituents (M2, S2, N2, K2, K1, O1, P1, Q1, MF, and MM). It is predicted by a tide model called TMD (Padman and Erofeeva 2004). Wind data and air pressure data are the Climate Forecast System Reanalysis (CFSR) data obtained from the National Centers for Environmental Prediction (NCEP). The resolution for the wind and air pressure data is 0.5°×0.5°with a time interval of 6 hours. Wind data are interpolated into the mesh grid.

Model-data comparison and Preliminary Results. The preliminary model-data comparison is shown in Figures A-3–A-6. It can be seen that the east component of the velocity was well captured by the model, but the north component was not. The reason could be the inaccuracy in bathymetry data. The model is currently being improved. Preliminary results of circulation under Hurricane Harvey is shown in Figures A-7–A-15.

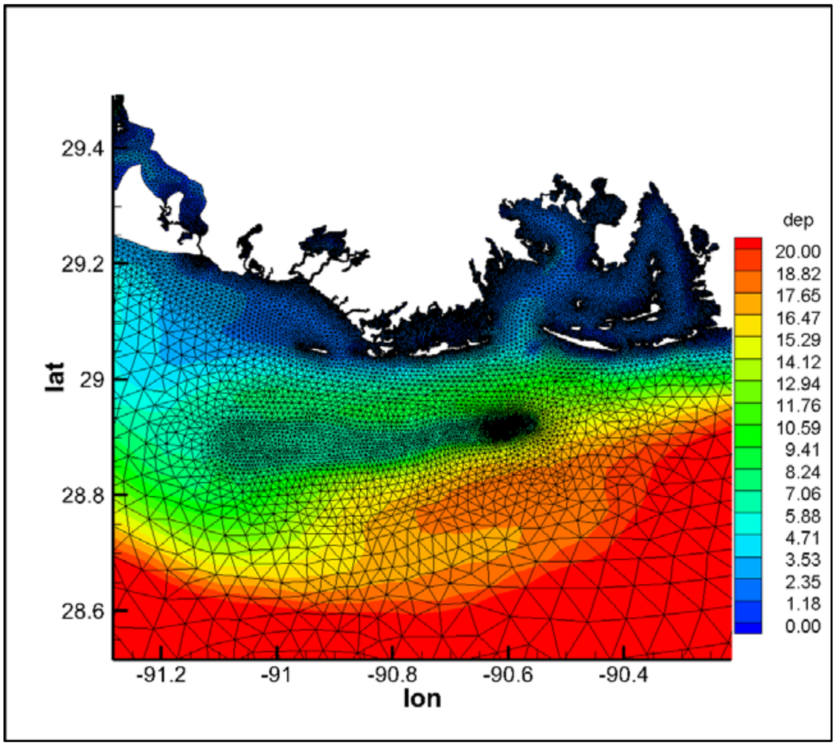

Figure A-2. Model grid zoomed in on the Ship Shoal area.

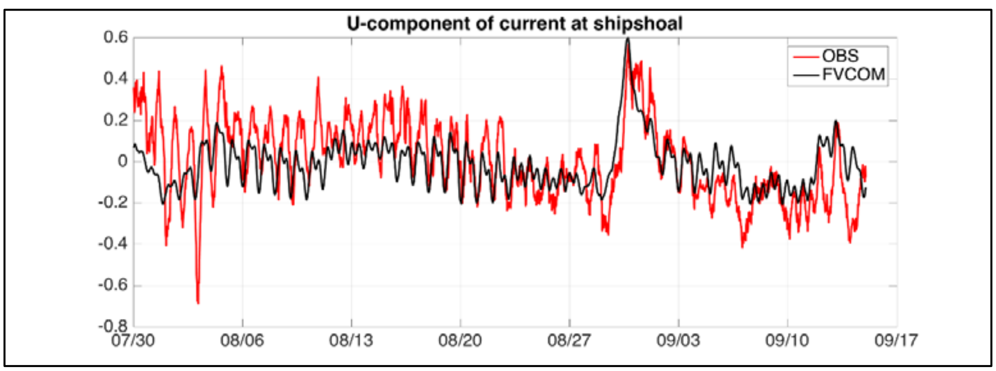

Figure A-3. Model comparison with observations from the Ship Shoal for the raw east component of the horizontal velocity.

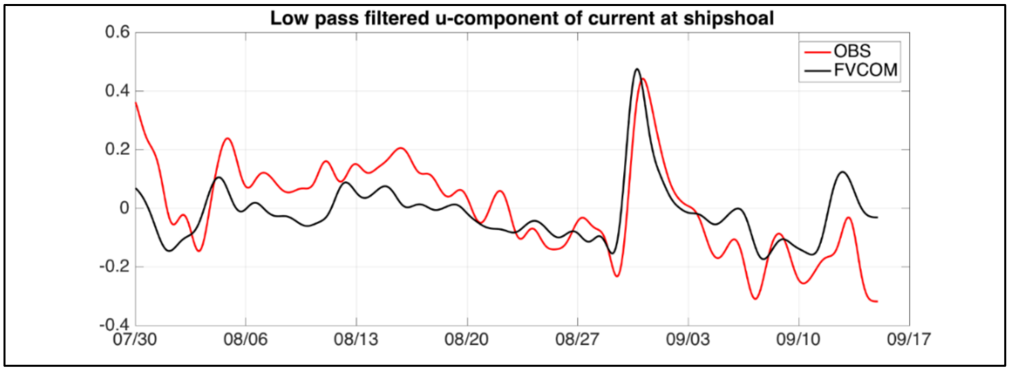

Figure A-4. Model comparison with observations from the Ship Shoal for the 40-hour low-pass filtered east component of the horizontal velocity.

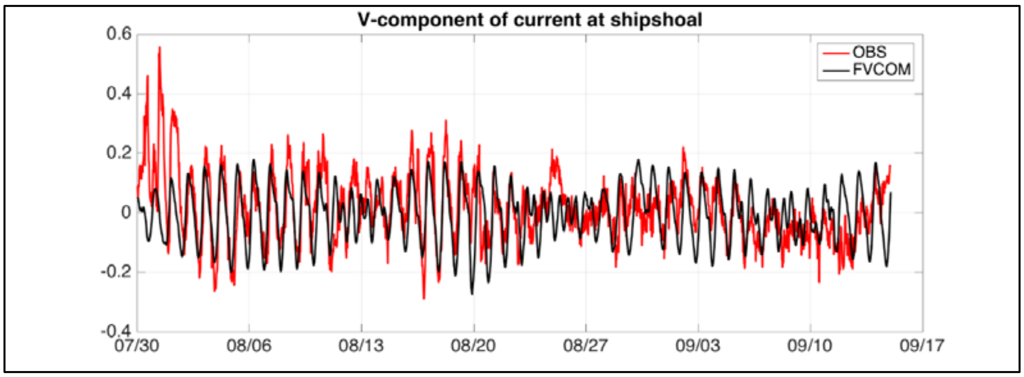

Figure A-5. Model comparison with observations from the Ship Shoal for the raw north component of the horizontal velocity.

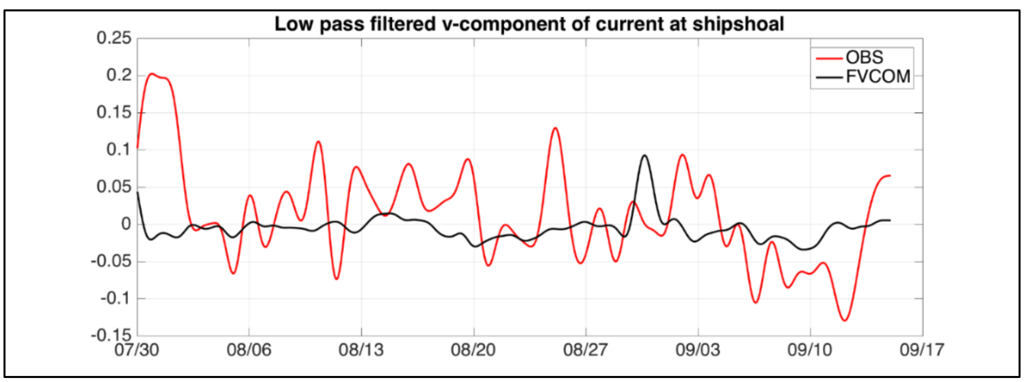

Figure A-6. Model comparison with observations from the Ship Shoal for the 40-hour low pass filtered north component of the horizontal velocity.

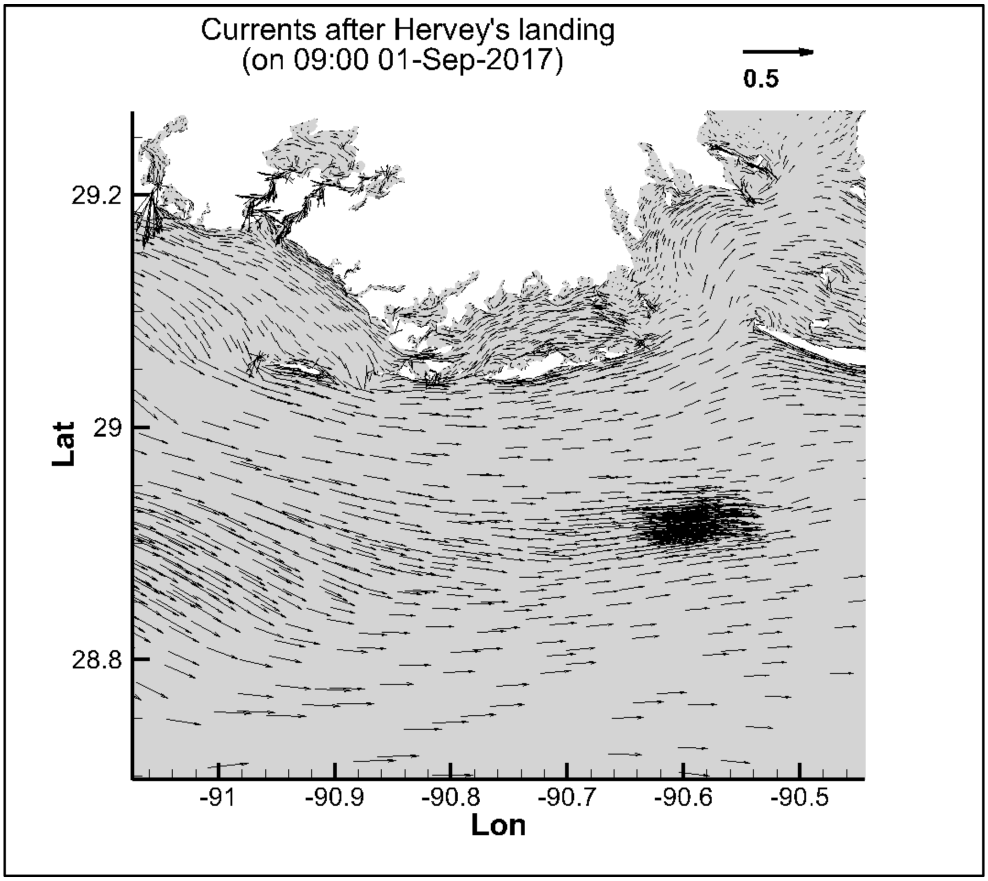

Figure A-7. Example flow field for Hurricane Harvey.

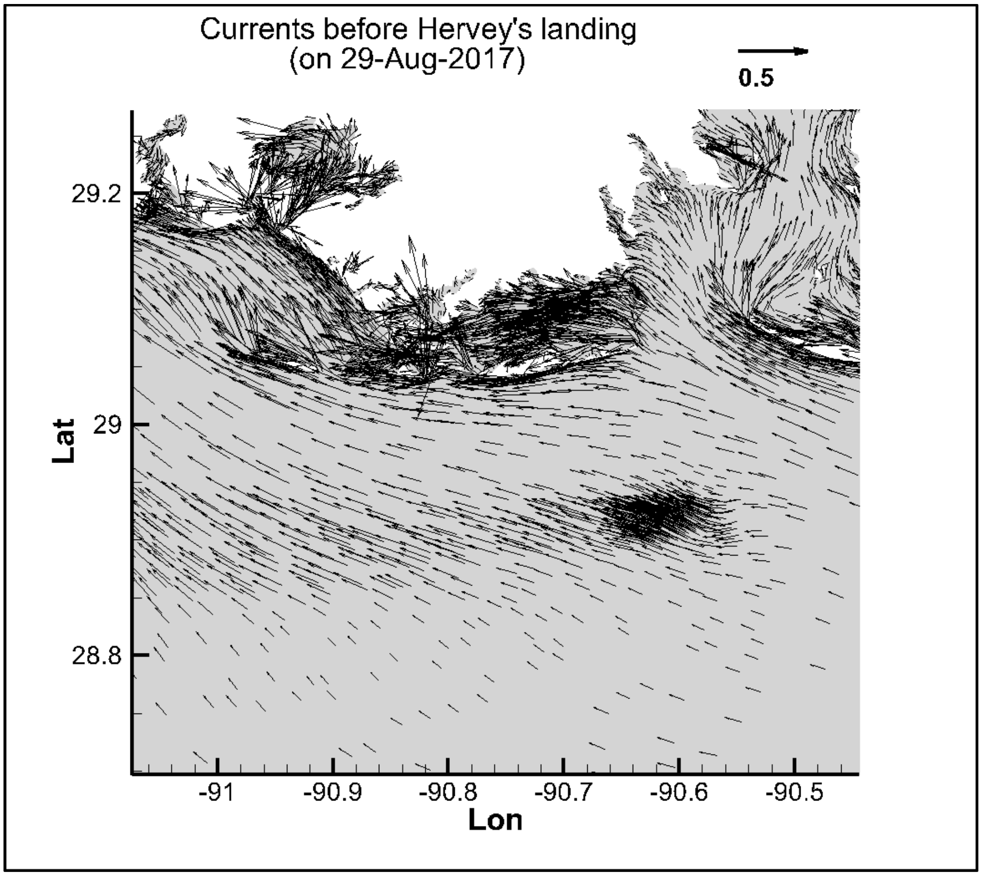

Figure A-8. Example flow field for Hurricane Harvey (continued).

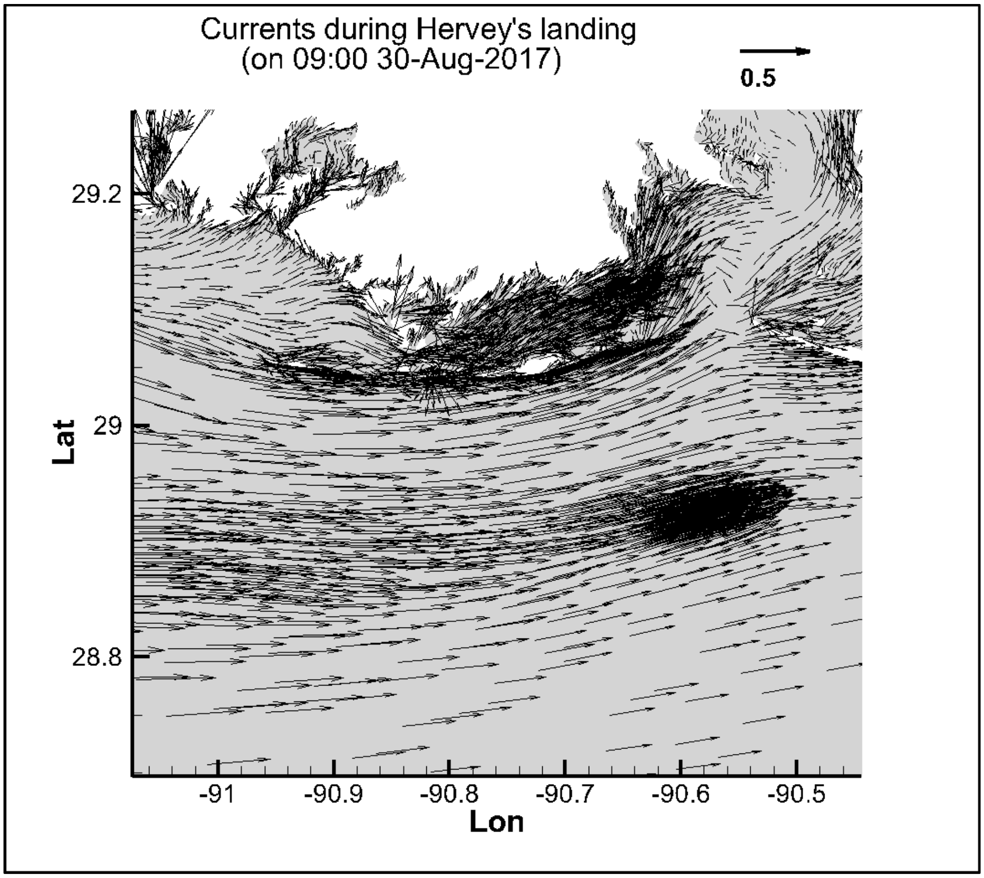

Figure A-9. Example flow field for Hurricane Harvey (continued).

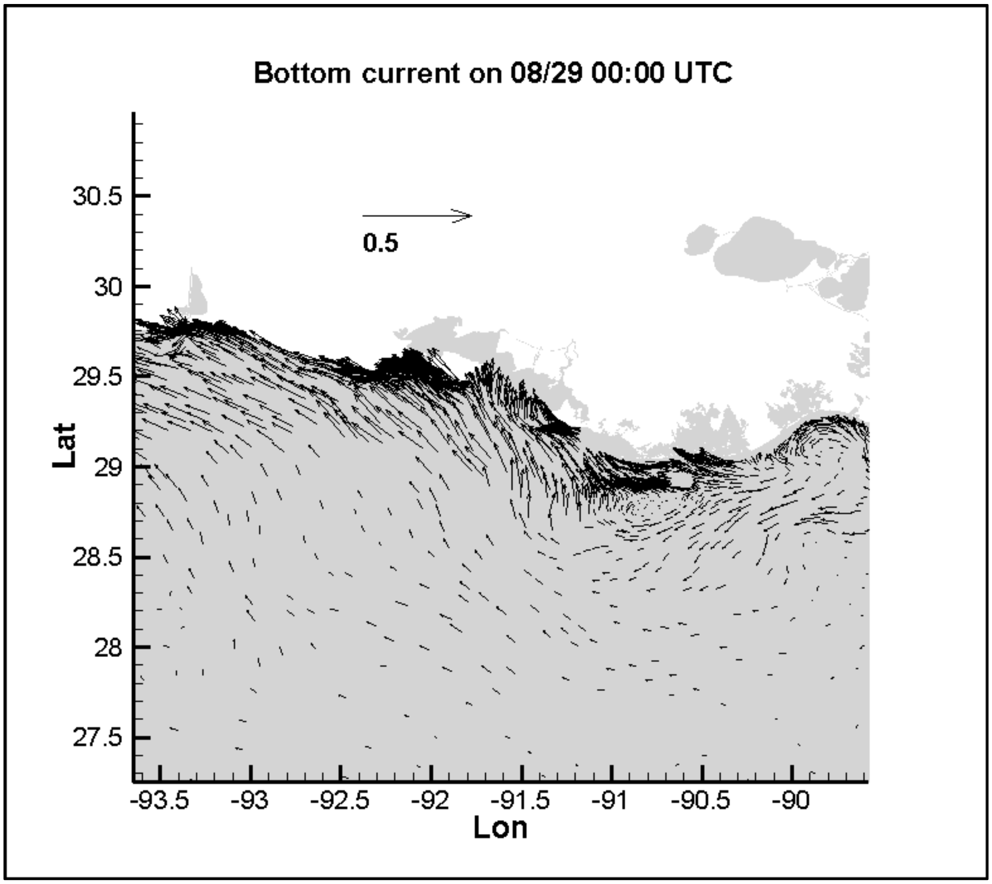

Figure A-10. Example flow field for Hurricane Harvey (continued).

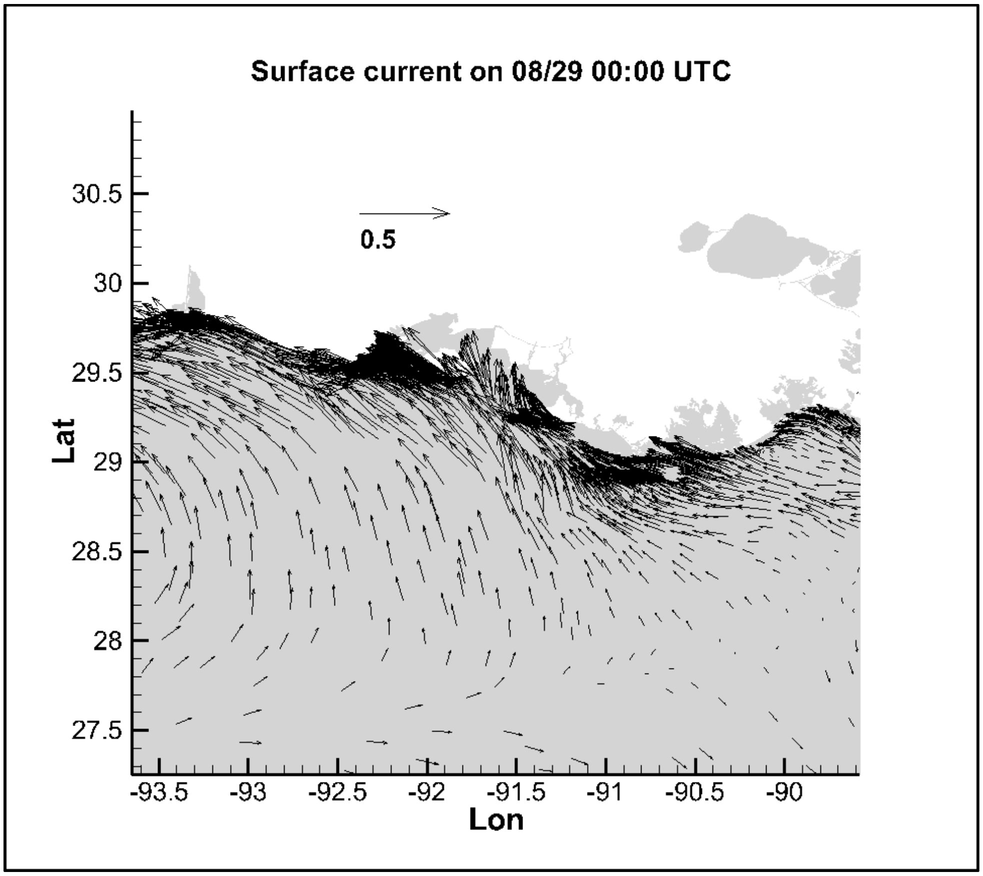

Figure A-11. Example flow field for Hurricane Harvey (continued).

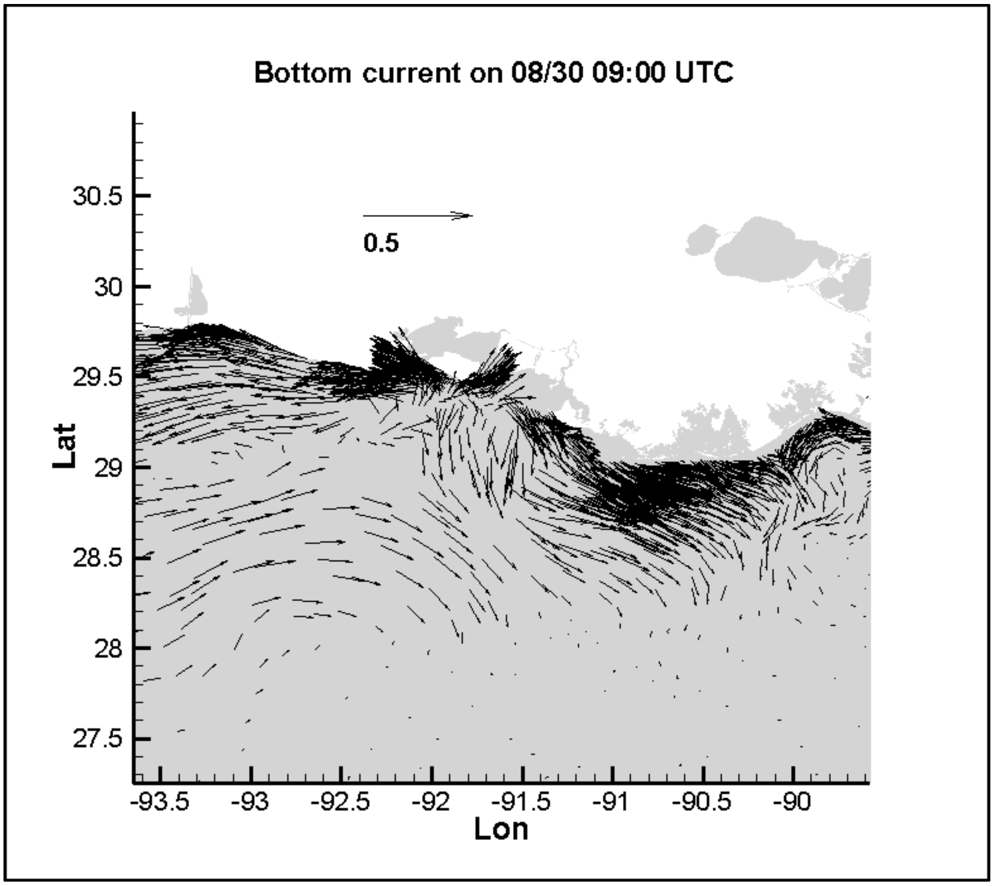

Figure A-12. Example flow field for Hurricane Harvey (continued).

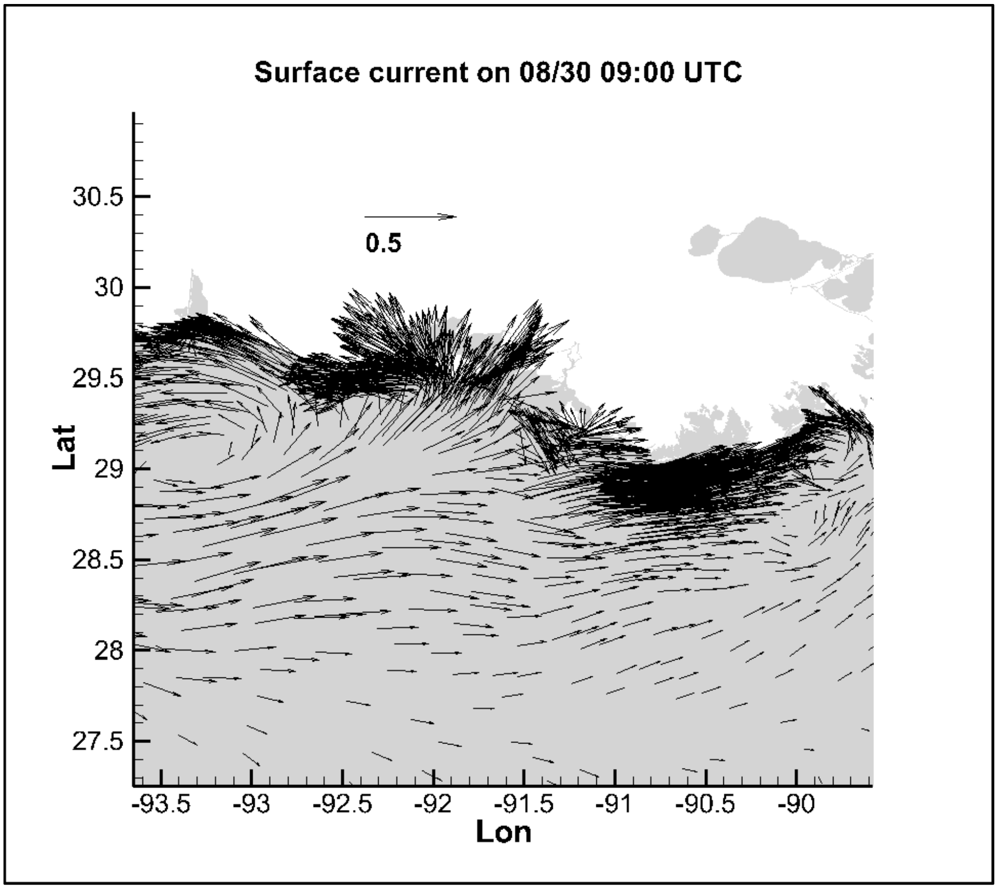

Figure A-13. Example flow field for Hurricane Harvey (continued).

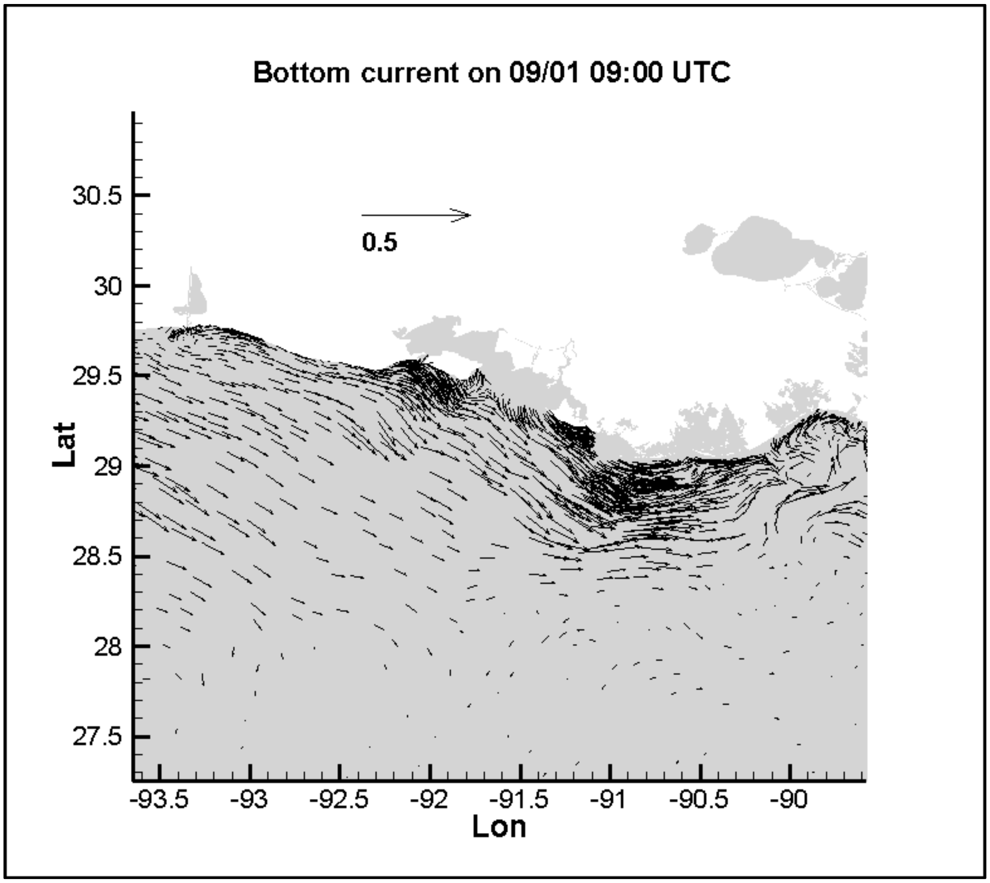

Figure A-14. Example flow field for Hurricane Harvey (continued).

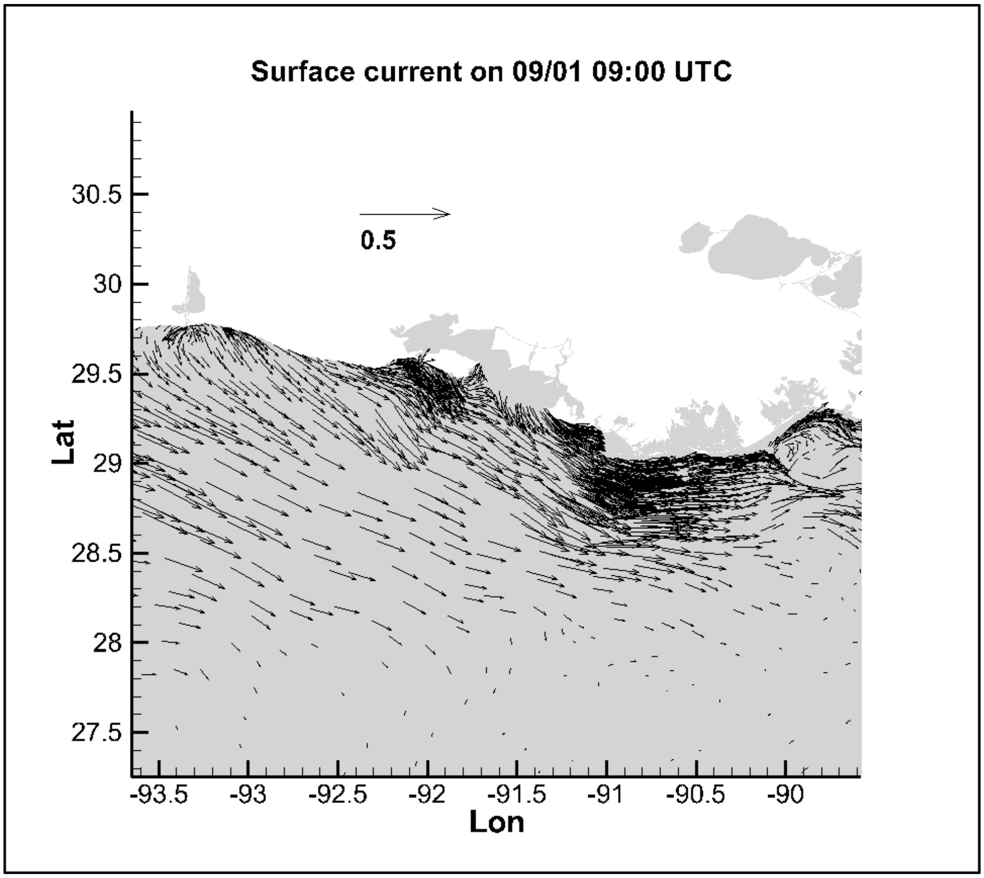

Figure A-15. Example flow field for Hurricane Harvey (continued).

Appendix 1 References

Padman L, Erofeeva S. 2004. A barotropic inverse tidal model for the Arctic Ocean. Geophys Res Lett. 31:L02303. doi:10.1029/2003GL019003

Department of the Interior (DOI)

The Department of the Interior protects and manages the Nation's natural resources and cultural heritage; provides scientific and other information about those resources; and honors the Nation's trust responsibilities or special commitments to American Indians, Alaska Natives, and affiliated island communities.

Bureau of Ocean Energy Management (BOEM)

The mission of the Bureau of Ocean Energy Management is to manage development of U.S. Outer Continental Shelf energy and mineral resources in an environmentally and economically responsible way.

BOEM Environmental Studies Program

The mission of the Environmental Studies Program is to provide the information needed to predict, assess, and manage impacts from offshore energy and marine mineral exploration, development, and production activities on human, marine, and coastal environments. The proposal, selection, research, review, collaboration, production, and dissemination of each of BOEM’s Environmental Studies follows the DOI Code of Scientific and Scholarly Conduct, in support of a culture of scientific and professional integrity, as set out in the DOI Departmental Manual (305 DM 3).